2020

Classifying Flow-kick Equilibria: Reactivity and Transient Behavior in the Variational Equation

Alanna Haslam

Classifying Flow-kick Equilibria: Reactivity and Transient Behavior in the Variational Equation

An Honors Paper for the Department of Mathematics

By Alanna Haslam

Bowdoin College, 2020

Acknowledgements

What you see here is the culmination of a year long project that has sparked my joy for mathematics more than I had thought possible. That is not to undermine the amount of joyful, enthusiastic moments of math I have shared between my peers and the Bowdoin math faculty during these past few years. To each of the Bowdoin math faculty, thank you for making my experience far better than I could have imagined.

In particular I want to thank: Prof. Broda for helping me to develop my mathematical communication skills and lending thought to many of the ideas in this thesis; Prof. Micheli for bringing me up through my first semester of college mathematics and encouraging me to continue pursuing mathematics with joy and enthusiasm; Prof. King for taking me under his wing the summer after my first year to help me learn set theory, logic, and proof writing while giving me a taste of algebra and number theory; Prof. Chong for teaching me how to build mathematical models and giving me my first taste of applied analysis and PDEs; Prof. Barker for teaching me real analysis in the most fun way I can imagine; Prof. O'Brien for helping me realize that stochasticity is actually pretty fun; and Prof. Pietraho for helping me see the coexistence of pure and applied mathematics.

To all of my mathematical peers who I've spent time huddled around a chalkboard with: thank you! It has been a real joy to engage with you and be challenged by the math we've done together.

For sharing this project with me, advising me in all things math and more, and inspiring me to be the math-loving person that I am today, I must thank Prof. Mary Lou Zeeman. Mary Lou has been a permanent fixture in my Bowdoin career. She started out as my first year advisor and I think even then I realized how lucky I was. Mary Lou is always prepared not just to offer math advise but to help coach me toward positive thinking and self-confidence. When I would ask what classes she thought I should take for the upcoming

semester, she would often reply by encouraging me to trust my interests and see what direction they would take me in. It has been such a pleasure to work with Mary Lou. I can't thank her enough for sharing dynamical systems with me and allowing me to follow my analytic interests throughout this project. I seriously doubt that I would have this much confidence and excitement starting my PhD next year without the encouragement and joy that Mary Lou has shared with me this year. I look forward to continue working with her in the future.

Finally, I must thank my family for their love and support. A huge thanks to my mom for encouraging me to become a strong, math-loving woman from an early age; to my dad for providing snorts of laughter and chewing gum my whole life; to my brother, Sam, for not getting his eyeballs stuck mid-roll despite me being home these past few months; and to Peter for loving me and reminding me to take time to be carefree. Thank you all.

Abstract

In light of concerns about climate change, there is interest in how sustainable management can maintain the resilience of ecosystems. We use flow-kick dynamical systems to model ecosystems subject to a constant kick occurring every τ time units. We classify the stability of flow-kick equilibria to determine which management strategies result in desirable long-term characteristics. To classify the stability of a flow-kick equilibrium, we classify the linearization of the time-τ map given by the time-τ map of the variational equation about the equilibrium trajectory. Since the variational equation is a non-autonomous linear differential equation, we conjecture that the asymptotic stability classification of each instantaneous local linearization along the equilibrium trajectory indicates the stability of the variational time-τ map. In Chapter 3, we prove this conjecture holds when all of the asymptotic and transient behavior of the instantaneous local linearizations is the same. To explore whether the conjecture holds in general, we ask: To what degree can transient behavior differ from asymptotic behavior? Under what conditions can this transient behavior accumulate asymptotically? In Chapter 4, we develop the radial and tangential velocity framework to characterize transient behavior in autonomous linear systems. In Chapter 5, we use this framework to construct an example of a non-autonomous linear system whose time-τ map has asymptotic behavior that differs from the asymptotic behavior of each instantaneous linear system that composes it. Future work seeks to determine whether this constructed example can arise as a variational equation, and thus provide a counterexample for our conjecture.

Contents

Chapter 1

Introduction to Flow-kick Systems

In recent years, the scientific community has become increasingly alarmed by current and projected reports of rapid climate change. Global warming, rising sea levels, melting ice caps, and increased frequency of extreme weather events threaten ecosystems which we are reliant on both for resources and for the sustained biodiversity of the planet [7]. In light of these growing concerns, there is renewed interest in investigating the role that sustainable management techniques could have in the resilience of ecosystems. How might regular intervention affect the natural stable states of ecosystems whose underlying behavior is being affected increasingly by changes in the climate? Having predicted the eventual extinction of a species if the current conditions persist, how might we subvert this eventuality by regular management of that species or its environment? Even if that disaster can be avoided, is the required intervention realistic? Is it possible to minimize the effort required to change the stable state of the system?

All of these questions and more can be addressed through a flow-kick modeling framework [8, 11, 9], a special case of impulsive differential equations [2, 1]. In short, flow-kick dynamical systems are used to model systems that exhibit continuous growth ("flow") interspersed by discrete changes ("kick"). Before defining what we mean precisely, let's set up an example to provide us with a concrete illustration of flow-kick systems at work.

1.1 A Gardening Example

To establish how to build a flow-kick model, suppose you have a vegetable garden which you tend during the beautiful summers of Maine. You may have a bed of peas. In this bed of peas it is inevitable that weeds will also want to grow. The weeds will benefit from the fertilizer, minerals, and water you put into your soil so that your peas will grow. The pea plants and the weeds growing in the same bed will naturally compete for resources. Perhaps, in recent years, the summers have been unnaturally hot and dry. You can keep watering your peas but the natural weather is just not ideal for them. Instead, the weeds are taking over; they don't seem to mind the heat.

Left only with your usual watering and fertilizing routine, the peas and weeds are growing according to a competition model. If we let P represent the size of the pea population and W represent the size of the weed population, we can represent their growth in relation to one another as a system of ODEs:

$$\begin{aligned} \frac{dP}{dt} &= r_p P\left(1 - \frac{P + \alpha_{wp} W}{k_p}\right) \\ \frac{dW}{dt} &= r_w W\left(1 - \frac{W + \alpha_{pw} P}{k_w}\right) \end{aligned} \tag{1.1}$$

In a Lotka-Voltera competition model as we see above, r_i represents the intrinsic per capita growth rate of species i, K_i represents the carrying capacity of each species, and α_{ij} represents the negative impact of species i on species j. Since weeds often grow faster and more densely, we will assume that $r_w > r_p$ and $k_w > k_p$. We will also assume that since peas are more delicate than weeds, the presence of the weeds would affect the growth of the peas more than the peas would affect the weeds (ie. $\alpha_{wp} > \alpha_{pw}$). For the purpose of simulation, let's assign these parameters values.

$$\begin{aligned} \frac{dP}{dt} &= 0.05P\left(1 - \frac{P + 3W}{8}\right) \\ \frac{dW}{dt} &= 0.15W\left(1 - \frac{W + P}{10}\right) \end{aligned} \tag{1.2}$$

As can be seen from the phase plane of this Lotka-Voltera model (see Figure 1.1),

the stable equilibrium of this system is extinction for the peas and growth to full carrying capacity for the weeds. Clearly this is not a desirable stable equilibrium. We want our peas to grow, if not to carrying capacity, than at least to the extent that they will produce some pods for us to enjoy.

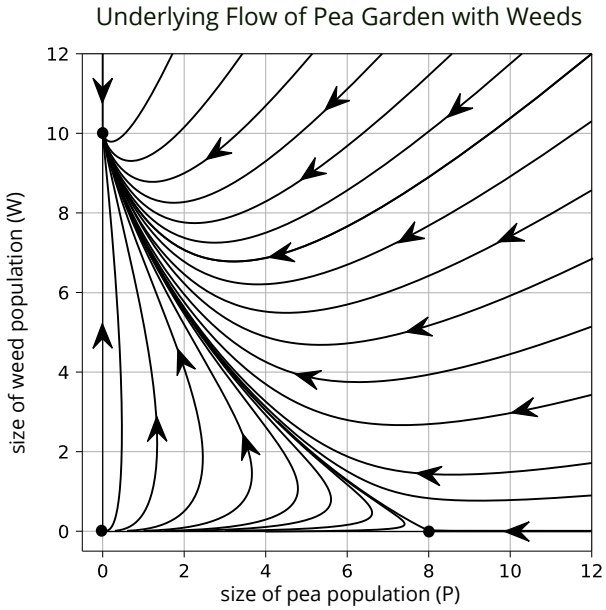

Figure 1.1: A phase portrait for the system of differential equations given in Equation 1.2. Though the natural attracting equilibrium is at $(0, 10)$, there are some regions of the phase plane where solutions are attracted temporarily to $(8, 0)$. Keeping our garden in this region is desirable.

The natural course of action would be to remove some amount of the weeds every couple of days.[1] This is not a continuous or gradual decrease in the size of the weed population, but a rapid decrease modeled as instantaneous. Thus if we were to chart the size of pea and

[1]In this case, it is conceivable that the size of the weed population prior to a weeding event is less than the fixed amount we had determined to weed. Weeding by this amount would then result in a negative population. This is clearly not realistic, however we do want our model to exhibit the regularity of a fixed weeding amount. For the sake of illustration, we will choose the initial values and predetermined weeding parameter such that this event does not occur. Note that there are similar dynamical systems in which we could model the same scenario but instead of removing a fixed amount, we could remove a fixed fraction of the weeds. For related work see [9, 11].

weed populations in our garden we would not have one smooth curve, but rather disjointed sections of smooth curve (see Figure 1.1). Such an altered system is what we mean when we say *flow-kick system*. The *flow* refers to the periods of natural, undisturbed growth and the *kick* refers to the regular weeding event.

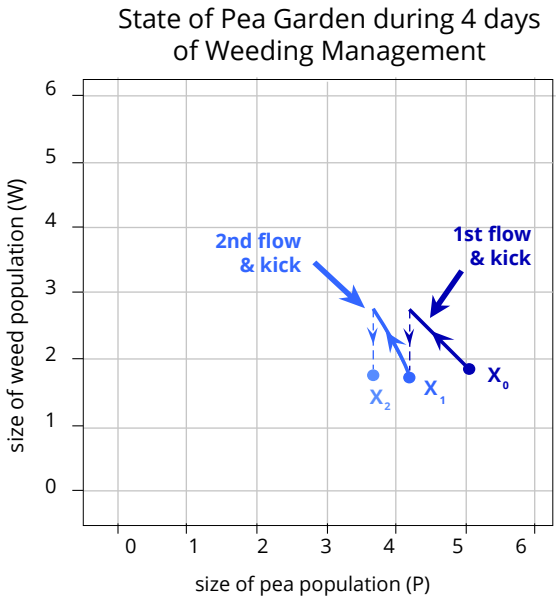

Figure 1.2: The two day periods between weeding events are represented by the smooth solid curves. Our weeding events themselves take "instantaneously" relative to the growth timescale are represented by the dashed lines. Pictured here are two iterations of this weeding regime if our garden starts in state X_0.

1.2 Defining Flow-kick Systems

Now that we have an intuitive example of what we mean when we say flow-kick system, we are ready to formalize this understanding. Before formally defining a flow-kick system, let's gather the materials that allow us to build the model.

Notation 1.1. Our recipe for a flow-kick dynamical system has three ingredients.

1. A system of ODEs that describes the continuous *flow* behavior:
$$\frac{dX}{dt} = F(X). \tag{1.3}$$
where $F \in C^1$ is a continuous, differentiable vector field. Note that here $X \in \mathbb{R}^n$ because we assume that the state of our model can have an arbitrary dimension n.

2. A flow time $\tau \in \mathbb{R}$. This describes how much time elapses between each kick. In other words, between each kick, the system flows for τ time units.

3. A kick vector $k \in \mathbb{R}^n$. This is the disturbance that occurs after each time-τ flow period. Note that k has the same dimension as X. This is because each component of k describes how the corresponding component of X gets shifted at the time of the kick.

With this notation we are now ready to define the *flow-kick map* which formally describes the behavior of a flow-kick system.

Definition 1.2. *Given a triple (F, τ, k) as in Notation 1.1,*

The **flow** $\phi(t, X_0) : \mathbb{R} \times \mathbb{R}^n \to \mathbb{R}^n$ *generated by $\frac{dX}{dt} = F(X)$ is the solution to $\frac{dX}{dt} = F(X)$ for all $t \in \mathbb{R}$ with initial condition $X_0 \in \mathbb{R}^n$.*

The **time-τ map** ϕ_τ *generated by $\frac{dX}{dt} = F(X)$ is given by*

$$\phi_\tau : \mathbb{R}^n \to \mathbb{R}^n$$
$$\phi_\tau : X_0 \mapsto \phi(\tau, X_0)$$

where $\phi(\tau, X_0)$ is the value of the flow at time τ.

The **flow-kick map** $G_{\tau,k}$ *is given by*

$$G_{\tau,k} : \mathbb{R}^n \to \mathbb{R}^n$$
$$G_{\tau,k} : X_0 \mapsto \phi_\tau(X_0) + k$$

where ϕ_τ is the time-τ map generated by $\frac{dX}{dt} = F(X)$.

Notice that the time-τ map takes an initial point and gives a snapshot of its location in state space after flowing for τ units of time. The flow-kick map describes what happens to a point after it has undergone a flow period of τ units as well as a kick.

Example 1.3. Recall our gardening example from Section 1.1.

What are the three ingredients from our example?

1. We already constructed a system of ODEs to model the underlying growth and competition of the two species. Therefore, this first component of the flow-kick system is given by Equation 1.2. Written in vector form, $X = \left(\begin{smallmatrix} P \\ W \end{smallmatrix}\right)$ and
$$\frac{dX}{dt} = \begin{pmatrix} \frac{dP}{dt} \\ \frac{dW}{dt} \end{pmatrix} = F(X) = \begin{pmatrix} 0.05P\left(1 - \frac{P+3W}{8}\right) \\ 0.15W\left(1 - \frac{W+P}{10}\right) \end{pmatrix}$$
2. We said that we would weed every couple of days. To make that precise, let $\tau = 2$ days.
3. Weeding means the removal of some weed biomass from the system. For the purpose of our model let's assume that we can always remove the exact same amount of biomass (say ω). Then the kick vector of the flow-kick system is given by $k = \left(\begin{smallmatrix} 0 \\ -\omega \end{smallmatrix}\right)$.

What is the flow-kick map?

$$G_{\tau,k}(X) = G_{\tau,k}\left(\left(\begin{smallmatrix} P \\ W \end{smallmatrix}\right)\right) = \phi_2\left(\left(\begin{smallmatrix} P \\ W \end{smallmatrix}\right)\right) + \left(\begin{smallmatrix} 0 \\ -\omega \end{smallmatrix}\right)$$

where ϕ_2 is the 2 day map derived from F.

If we know that the biomass of the peas and weeds are currently P_0 and W_0 respectively, then $G_{\tau,k}\left(\left(\begin{smallmatrix} P_0 \\ W_0 \end{smallmatrix}\right)\right)$ tells us the biomass of the peas and weeds after two days of growth and one weeding session.

Now that we have a clear understanding of the components that make up our flow-kick model and the formal definition of the flow-kick map, we are ready to formally define a flow-kick system using the language of discrete dynamical systems [5].

Definition 1.4. *Given a triple (F, τ, k), the* **flow-kick system** *associated with that triple is defined by iterating the flow-kick map $G_{\tau,k}$. For each initial condition $X_0 \in \mathbb{R}^n$, $X_{n+1} = G^n_{\tau,k}(X_0)$.*

The sequence obtained by iterating the flow-kick map with initial value X_0 is called the **flow-kick orbit**. *The initial value X_0 is called the* **seed** *of the orbit.*

The flow-kick system consists of iterations of the flow-kick map $G_{\tau,k}(X_n)$. One way of describing this is as the collection of the obits generated by all possible seeds $X_0 \in \mathbb{R}^n$. One flow-kick orbit fully describes what would happen to the state of the system we are modeling if it started out at X_0 and then continued to be flowed and kicked for all time under (τ, k) management.

Example 1.5. To fix our ideas, let's go back to our gardening example.

It's early July so your garden is just getting started. It's becoming apparent that you need to do something about those weeds if the peas are going to survive. You decide to weed every τ days, every time removing a fixed amount of weeds.

Because you love your garden, you are excited to see the progress of your garden and you are careful to record the state of your garden after every weeding session. This record is the orbit.

We can describe what happens under the dynamics of flowing and kicking by solely looking at the obits, that is the the discrete sequences of post-kick points. During the periods between kicks, the solution flows through state space according to the vector field F. That behavior is implicit in the flow-kick map. However, having an explicit way of talking about these flow periods is useful and, as such, we will establish language for them in Definition 1.6.

Definition 1.6. *Given a triple* (F, τ, k)

The **time-τ trajectory** *of a single point X_n in a flow-kick orbit describes the path taken through state space during* $[0, \tau]$ *according to the underlying dynamics of the system. It is given by:*

$$\phi(t, X_n)\Big|_{0 \le t \le \tau}$$

Given a seed X_0, the **flow-kick trajectory** *is the sequence of time-τ flows corresponding to each point in the flow-kick orbit.*

$$\bigcup_{n=0}^{\infty} \phi(t, X_n)\Big|_{0 \le t \le \tau}$$

In essence, the flow-kick trajectory is a continuous-time view of the orbits that make

up our flow-kick system. For a summary of all of the ways we describe the dynamics of the flow-kick system, see table 3.1.

Term	Definition	Description
time-τ map $\phi_\tau(X)$	1.2	Input is a point, output is where that point will be after flowing for τ time.
flow-kick map $G_{\tau,k}(X)$	1.2	Input is a point, output is where that point will be after flowing for τ time and being kicked.
flow-kick orbit $\{G^n_{\tau,k}(X)\}^\infty_{n=0}$	1.4	The sequence of post-kick points originating an initial condition (seed) X_0.
time-τ trajectory $\phi(t, X)\|_{0\le t\le\tau}$	1.6	The smooth curve from X to $\phi_\tau(X)$ obeying differential equation 1.3.
flow-kick trajectory $\bigcup^\infty_{n=0}\phi(t, X_n)\|_{0\le t\le\tau}$	1.6	The sequence of time-τ flows originating at each point in the flow-kick orbit.

Table 1.1: A summary of the many ways we talk about the dynamics of a flow-kick system.

Example 1.7. Continuing our gardening example, remember that if you keep a record of the state of your garden after every weeding session you will have orbit of that flow-kick system. If you were to try and collect the data to describe the flow-kick trajectory, you would need to set up a magical measurement device that continually measures and records the biomass of peas and weeds at all hours of every day. You would still measure your garden after weeding but you would also have a record of what happened at every moment in between. (See Figure 1.2).

The flow-kick orbit and the flow-kick trajectory are two ways to approach the same model. Both give a record of the behavior of the system over time, but the flow-kick trajectory yields a more explicit record of the behavior of the system in time and space.

From an applied perspective, the flow-kick trajectory can be very useful as it addresses the health of the system in between, as well as directly, after each kick. It is often the case that we care about the system being in a healthy state not just immediately after the kicks. For example, an insulin-dependent diabetes patient may have healthy blood-sugar level immediately after taking their regular dose of insulin, however it is important that this blood-sugar level also stays within a healthy target range between doses.

From a theoretical perspective, the flow-kick trajectory carries important information

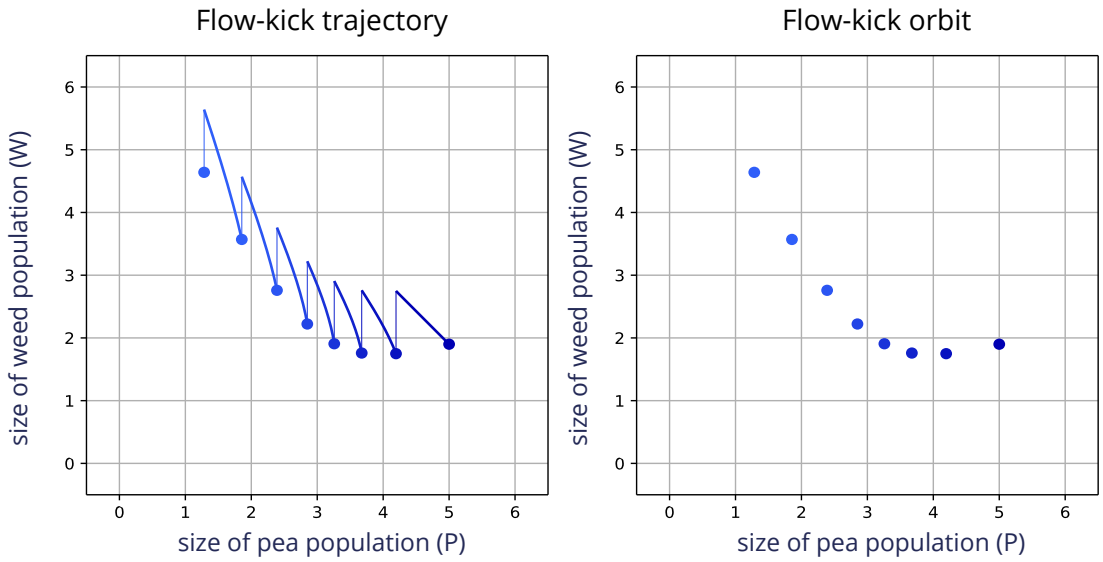

Figure 1.3: Both figures describe how our population of peas and weeds changes under the dynamics of Equation 1.2 subject to our prescribed weeding regimen. (a) The flow-kick trajectory shows how solutions move in state space for all moments of continuous time. The post-kick point is represented as a point at the beginning of each flow-trajectory. (b) The flow-kick orbit keeps a record of all the post-kick points.

about the behavior of the system that is implicit in the flow-kick orbit. Though observation of the post-kick points does say a lot about the long-term behavior of the system, one of the biggest factors that drives this actual behavior is the underlying flow. The output of the flow-kick map is dependent on solving the underlying flow. Implicit in the map $G_{\tau,k}(X_0) = X_1$ is the continuous instruction that the vector field F gives at each point in the time-τ flow. X_0 cannot get to X_1 without the influence of all of the points along the flow. For this reason, as we will see in Chapter 2, the flow-kick trajectory is central to our analysis of what classifies the behavior of the flow-kick system.

1.3 Flow-kick Equilibria

A primary way that we can understand more about how solutions to a flow-kick system behave, is by looking for solutions that are fixed in place by the dynamics of our flow and kick. Solutions that are invariant under the dynamics of the flow-kick map (equilibrium

solutions) or that belong to sets that are invariant under the flow-kick map (periodic orbits and other types of steady state solutions) provide landmarks in state space to describe what kind of behavior may be expected from other solutions.

In particular, we will look at equilibrium solutions as a way of determining what kinds of flow-kick management can help to achieve desirable long-term behavior in any given system that we are modeling. This type of application of flow-kick systems is called decision support. We will discuss how it motivates our study of flow-kick systems in greater detail in Section 1.4.

One benefit of looking at equilibrium solutions is that it is an analytic method can be generalized to many flow-kick systems at once. For example, we can think about the one particular flow-kick model that we used in Example 1.3, or we can think about all flow-kick systems that can arise from the ODE model of our pea garden, or we can think about all flow-kick systems that arise by applying flow-kick management to general Lotka-Voltera competition models.

Definition 1.8. *Given a triple (F, τ, k). A point $X^* \in \mathbb{R}^n$ is a* **flow-kick equilibrium** *if and only if it is a fixed point of the flow-kick map. That is, if and only if*

$$X^* = G_{\tau,k}(X^*)$$

The corresponding **flow-kick equilibrium trajectory** *is the time-τ flow trajectory originating at the equilibrium point:*

$$\phi(t, X^*)\Big|_{0 \le t \le \tau}$$

Given a (F, τ, k), the above definition does not give us a way to *find* flow-kick equilibria, which is, in general, a non-trivial task. With an applied focus on decision support, however, we often consider a large set of flow-kick systems all with the same underlying vector field $F \in C^1$. Given a two parameter family of flow-kick systems corresponding to (F, τ, k) with $\tau \in \mathbb{R}$ and $k \in \mathbb{R}^n$ as parameters, the following lemma and corollary state that any $X^* \in \mathbb{R}^n$ is a flow-kick equilibrium in the family of systems. Given F and a choice of (τ, X^*) there is a k to make X^* an equilibrium of (F, τ, k).

Lemma 1.9. *Given a vector field $F \in C^1$, a flow time τ, and a point in state space $X^* \in \mathbb{R}^n$, there exists a kick vector $k \in \mathbb{R}^n$ such that $X^* = G_{\tau,k}(X^*)$ is an equilibrium solution to the flow-kick system.*

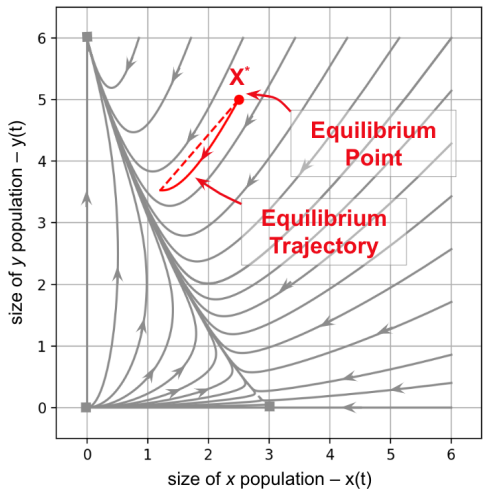

Figure 1.4: The underlying flow of the Lotka-Voltera competition model given in Example 1.11. Pictured in red is an equilibrium $X^* = (2.5, 5)$ of the flow-kick system when $\tau = 10$ and $k = (1.32, 1.47)$. Notice the distinction between the equilibrium point X^* and the equilibrium trajectory $\phi(t, X^*$ for $t \in [0, \tau]$.

Proof. We are given a vector field F and a flow time τ. Thus we can construct a time-τ map ϕ_τ. Let $k = X^* - \phi_\tau(X^*)$. Then,

$$\begin{aligned} G_{\tau,k}(X^*) &= \phi_\tau(X^*) + k \\ &= \phi_\tau(X^*) + X^* - \phi_\tau(X^*) \\ &= X^* \end{aligned}$$

Therefore, X^* is a flow-kick equilibrium of the flow-kick system associated with (F, τ, k). □

Corollary 1.10. *Given a vector field $F \in C^1$, all points in state space $X \in \mathbb{R}^n$ are flow-kick equilibria under some management regime (τ, k).*

Example 1.11. To fix our ideas, let's introduce another example model of underlying flow. This Lotka-Voltera competition model will be used for our examples and figures for the

remainder of the thesis. It is given by:

$$\frac{dX}{dt} = F(x,y) = \begin{pmatrix} f(x,y) \\ g(x,y) \end{pmatrix} = \begin{pmatrix} 0.09x\left(1 - \dfrac{x-y}{3}\right) \\ 0.18y\left(1 - \dfrac{y-2x}{6}\right) \end{pmatrix}$$

Notice that this competition model is similar to our peas and weeds model. Here, just like the weeds, population y has a stronger intrinsic per capita growth rate and a larger carrying capacity than the other population. However, unlike in our peas and weeds example, the population with the weaker population dynamics overall (the peas/population x) has a stronger negative effect on the stronger population (the weeds/population y) rather than vice versa.

We can think of this model as corresponding to the interaction between competing native and exotic species of grass. The exotic species, y, has a stronger capacity for growth than the native species, x, however, species x is better at exploiting the resources around it. Thus, the presence of the native species x (and the corresponding decrease in the available resources) has a stronger negative impact on the exotic species y than vice versa.

In Figure 1.3, we see that the underlying flow has equilibria at (0,0), (0,6), and (3,0). Undisturbed, this grasslands ecosystem would see the extinction of the native grass and the full growth to carrying capacity of the exotic grass. We also see in Figure 1.3 that a flow-kick management pattern of $\tau = 10$, $k = (1.32, 1.47)$ yields a flow-kick equilibrium at $(2.5, 5)$.

Suppose that we still $\tau = 10$ so our management of the system will take place every 10 units of time, but we'd prefer the flow-kick equilibrium to show more of a balance between the native and exotic grass species. By Corollary 1.10, this is not a problem! Any state (x^*, y^*) can be a flow-kick equilibrium if we pick the kick management that balances how much the grass populations will change over the 10 time units.

For example, let's say we want our grasses species to balance at a flow-kick equilibrium of $X^* = (4, 4.2)$. How do we find the kick k for which this occurs? First we observe that if the system starts at $X_0 = (4, 4.2)$ then after 10 units of their uninterrupted, natural dynamics, the population of grass x will be measured by 1.96 and the population of grass y

will be measured by 2.3. We want to pick $k = (x_k, y_k)$ so that this flow balances:

$$(1.96, 2.3) + (x_k, y_k) = (4, 4.2)$$
$$\implies \quad (x_k, y_k) = (4, 4.2) - (1.96, 2.3) = (2.04, 1.9)$$

Thus $X^* = (4, 4.2)$ is a flow-kick equilibrium under $G_{\tau,k}$ if $\tau = 10$ and $k = (2.04, 1.9)$. This process is illustrated in Figure 1.3.

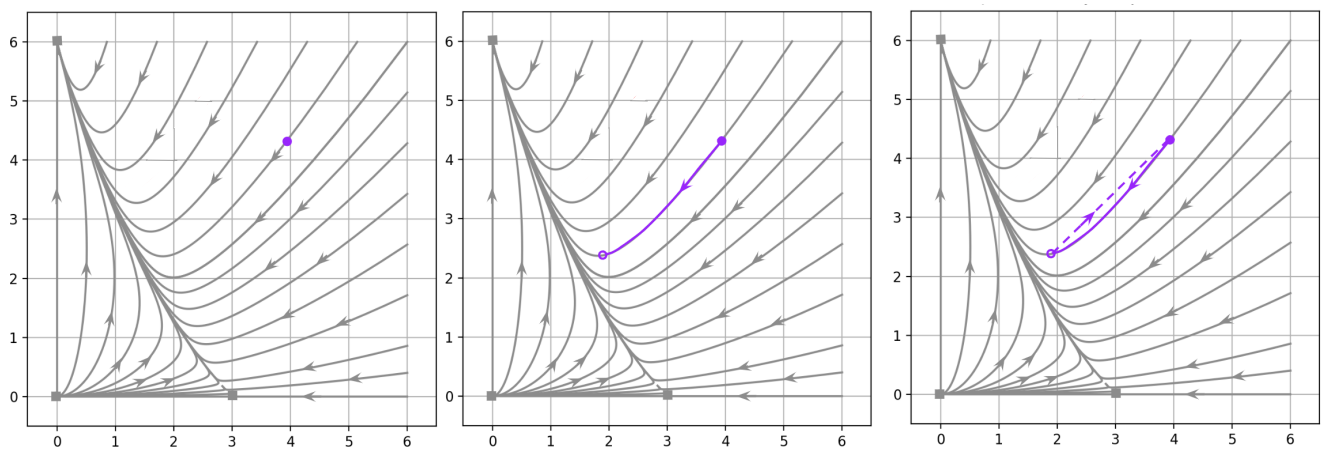

Figure 1.5: (a) We pick a point $(4, 4.2)$ that we want to have as a flow-kick equilibrium. (b) We flow for a period of $\tau = 10$ time units from the point $(4, 4.2)$ to the point $(1.96, 2.30)$ (c) We construct the kick k so that we end up right back at $(4, 4.2)$. Now the point $(4, 4.2)$ is a flow-kick equilibrium of the flow-kick map $G_{\tau,k}$.

Now that we know that any point in state space *can* be an equilibrium, we want to know which equilibria are important in predicting the long term behavior of a system or identifying a management regime that results in desirable behavior. This can be determined in two ways.

First, when working closely with an expert in the area of application, it may be possible to narrow down which region(s) of state space are desirable for the application in question. In that case, the analysis can be tailored to exploring management regimes that result in a desirable equilibrium trajectory.

Another way of determining the importance of an equilibrium is by characterizing it as

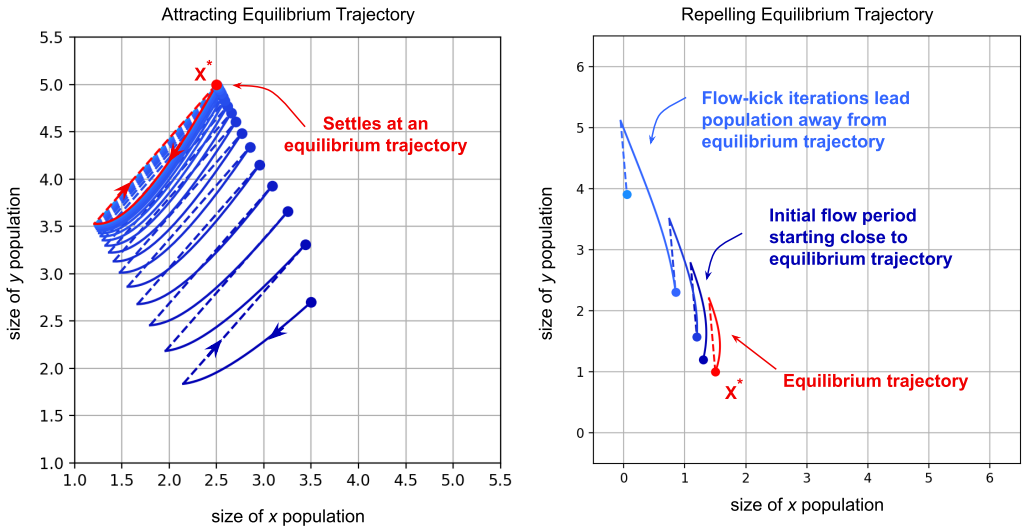

Figure 1.6: (a) A flow-kick equilibrium is attracting when nearby solutions get closer and closer to it as they keep getting iterated through the flow-kick map. (b) A flow-kick equilibrium is repelling if the flow-kick map takes points close to the equilibrium to points further away from the equilibrium.

either attracting or repelling nearby solutions in time. If an equilibrium is attracting then there will exist some basin of attraction in which solutions will asymptotically reach that equilibrium state (see Figure 1.3). If this attracting equilibrium is also desirable (as the application might require), then you may have found a management regime that forces the application system into a desirable behavior pattern.

This task of classifying equilibrium will become our primary focus. We will come back to it in greater detail in Chapter 2.

1.4 Motivational Goals

As mentioned in Section 1.3, one of the central applications of flow-kick systems is decision support for ecological management. In such situations we presume to be modeling a general ecological system in which humans wish to drive the natural behavior to a desirable equilibrium means of regular management.

An example to this type of application is found in Andrew Brettin's undergraduate thesis [4]. Brettin applied data collected by the University of Minnesota at the Cedar Creek Ecosystem Science Reserve to build a flow-kick model of how native and exotic grass species interact under various haying patterns. By simulating this model and varying its parameters, he explored the relative degree of success that various management regimes would have in re-stabilizing the native species of grass, maintaining biodiversity, and counteracting the effects of nutrient loading.

Brettin's work is an excellent example of how flow-kick systems can be used to analyze dynamic behavior at the scale of an individual ecosystem. This analysis could be generalized to the scale of all grassland ecosystems, leading us to ask how the general dynamic structures present in grasslands may suggest one or another general type of management. Abstracting to the next scale, we could ask how the structure of inter-species competition interacts with potential management strategies.

Another application of flow-kick systems is the measurement of resilience in ecosystems subject to disruption. In this framework, the regular kicks don't represent management strategies, but rather disturbances caused by climate change or other 'unnatural' changes in the ecological landscape. Instead of asking what combinations of τ and k recover the resilience of a system, we ask how much wiggle room a system has to flow-kick disturbances.

An example of this framework is Kate Meyer's work in one dimension [9]. Instead of measuring the basin of attraction in state space of a natural stable equilibrium to quantify resilience, she works in parameter space and measures how much of (τ, k) "disturbance" space causes flow-kick solutions to settle within the basin of attraction of the underlying equilibrium. While decision support applications lead to questions about how to find a particular desirable (τ, k) pair, the resilience approach to flow-kick systems leads to questions about the general behavior arising from large regions of (τ, k) disturbance space.

Because of the general treatment of disturbance space in the resilience framework, it is not sufficient to test a few (τ, k) candidates. Developing a complete resilience metric in this way requires full analytic classification of disturbance space. Though this paper will describe classification analysis primarily from the perspective of decision support, much of the work also contributes to the goal of attaining a resilience metric in higher dimensions.

Chapter 2

Linearization of Flow-kick Systems

2.1 Introduction to Linearization

As we established in Chapter 1, there are two big picture goals to motivate us: decision support for ecological management and the development of a resilience metric that takes real, continued disturbance into account. From these two motivational goals, we established a primary working goal: to analytically characterize the behavior of flow-kick dynamical systems. More specifically, our goal is to classify the stability of flow-kick equilibrium.

Remark. Though we are primarily focused on equilibrium points in the flow-kick orbit, there may be other types of steady state solutions (eg. periodic solutions, limit cycle, etc.) that could describe the long-term behavior of flow-kick systems. These could be explored in future research to further expand the toolbox of analytic techniques for classifying the long-term behavior of flow-kick systems. The research presented here focuses on expanding that toolbox through studying the classification of equilibria.

Given a flow-kick system generated by (F, τ, k) and a flow-kick equilibrium X^* of that system, our task then is to determine whether X^* is an attracting equilibrium, a repelling equilibrium, or a saddle equilibrium. This will tell us whether, under (τ, k) management, X^* is a viable prediction of the long-term state of the system.

Language 2.1. In Chapter 3 we will establish how to characterize the stability classification of an equilibrium formally. For now, we will present an intuitive explanation of stability and introduce the language of stability that we will use through this and later chapters.

Recall that at an equilibrium, the dynamics of the system balance to achieve no change. The *stability classification* of an equilibrium refers to how stable that balance is.

If the system is balanced at the equilibrium and small perturbations in any direction don't affect that balance very much, the equilibrium is *stable*. This is like a ball sitting at the bottom of a bowl; it can be pushed in any direction and will still settle at equilibrium. For this reason, a stable equilibrium is also called a *attracting* equilibrium or a *sink* equilibrium.

If the system is balanced at the equilibrium but becomes more and more unbalanced if it is perturbed by even a small amount, then the equilibrium is *unstable*. You can imagine a ball balancing on top of a hill; if it is pushed just a little it will be repelled from its resting position at the top of the hill.

Note that in higher dimensions an equilibrium could be unstable in a variety of ways. Imagine the ball on top of a hill again; a nudge in any direction will cause the ball to be repelled from the equilibrium. Such an unstable equilibrium is referred to as a *repelling* equilibrium or a *source* equilibrium.

You could also imagine a ball sitting in the middle of a riding saddle. The equilibrium in the middle of the saddle is unstable because if you push the ball towards the side of the horse it will fall off. However, if you could push the ball precisely towards the horse's head it would (in theory) eventually return to the middle of the saddle, showing that the equilibrium is attracting in one direction. This type of unstable equilibrium is called a *saddle* equilibrium.

The process of classification begins with linearization of the system about the equilibrium (in both discrete and continuous dynamical systems). The aim is to determine whether solutions nearby the equilibrium tend toward the equilibrium or away from the equilibrium. Linearization is a natural way to approximate this local behavior so as to simplify the problem.

Recall from Definition 1.4 that the flow-kick orbit with seed $X_0 \in \mathbb{R}^n$ is generated by the following difference equation:

$$X_{n+1} = G_{\tau,k}(X_n) \tag{2.1}$$

To linearize the equilibrium X^*, we consider a nearby seed $X_0 \in \mathbb{R}^n$ that has some perturbation $U_0 \in \mathbb{R}^n$ from X^*. The seed can then be expressed as $X_0 = X^* + U_0$ and the orbit $X_n = G^n_{\tau,k}(X_0)$ can be expressed as $X_n = X^* + U_n$. By Equation 2.1 we also know that the orbit satisfies:

$$X_{n+1} = X^* + U_{n+1} = G_{\tau,k}(X_n) = G_{\tau,k}(X^* + U_n) \tag{2.2}$$

The linearization of this expression is merely the first order Taylor approximation of $G_{\tau,k}(X_n) = G_{\tau,k}(X^* + U_n)$ centered around X^*. Thus we can write:

$$\begin{aligned} X_{n+1} = X^* + U_{n+1} &= G_{\tau,k}(X_n) = G_{\tau,k}(X^* + U_n) \\ &\approx G_{\tau,k}(X^*) + D[G_{\tau,k}(X^*)]((X^* + U_n) - X^*) \\ &= X^* + D[\phi_\tau(X^*) + k]\,(U_n) \\ &= X^* + D[\phi_\tau(X^*)]\,(U_n) \\ \implies U_{n+1} &\approx D[\phi_\tau(X^*)]\,(U_n) \end{aligned} \tag{2.3}$$

where D represents the spatial derivative operator.

Equation 2.3 means that the linearization of the flow-kick map *is* the linearization of the time-τ map. In other words, the linear approximation of how perturbations evolve through one iteration of flow and kick is the same as the linear approximation of how perturbations evolve through one iteration of flow. Intuitively this makes sense since adding the same kick to both $\phi_\tau(X)$ and $\phi_\tau(X^*)$ does not effect their relative distance (see Figure 2.1). Lemma 2.2 makes this explicit: the kick has no role in determining the evolution of perturbations from the equilibrium trajectory under the dynamics of the flow-kick map.

Lemma 2.2. *Let* $X_{n+1} = X^* + U_{n+1}$. *Then* $U_{n+1} = X_{n+1} - X^* = \phi_\tau(X_n) - \phi_\tau(X^*)$.

Proof.

$$\begin{aligned} X_{n+1} - X^* &= G_{\tau,k}(X_n) - G_{\tau,k}(X^*) \\ &= \phi_\tau(X_n) + k - (\phi_\tau(X^*) + k) \\ &= \phi_\tau(X_n) - \phi_\tau(X^*) \end{aligned}$$

□

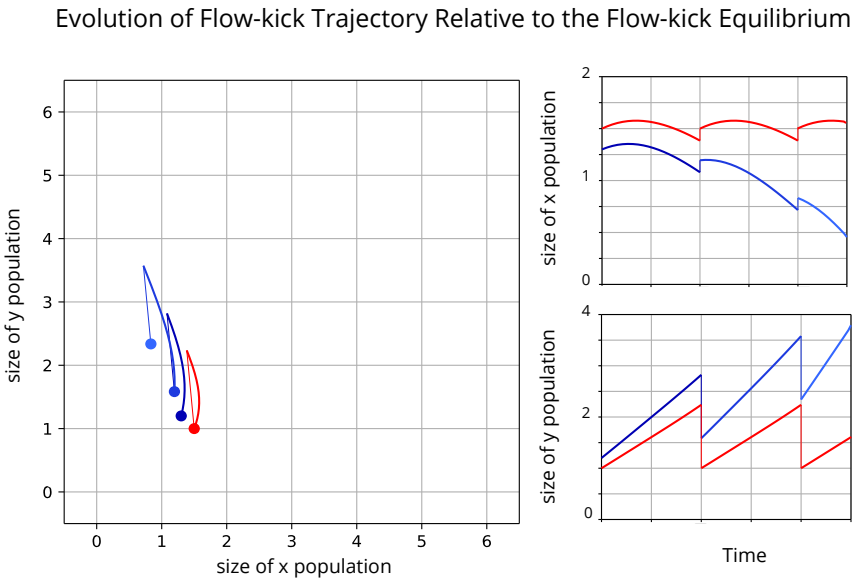

Figure 2.1: (a) As solutions nearby an equilibrium undergo flow-kick dynamics, they evolve relative to the equilibrium trajectory. The kick part of the flow-kick dynamics does not change this relative distance. (b) We see that the x distance between a solution (in blue) and the equilibrium solution (in red) changes during the time-τ flow but is unaffected by the kick. (c) Similarly the y distance between a solution and the equilibrium solution is unaffected by the kick.

Lemma 2.2 confirms that the way solutions behave relative to the equilibrium trajectory under flow-kick dynamics is unaffected by the kick. Thus both Equation 2.3 and Lemma 2.2 indicate that the linearization of the flow-kick map is obtained by linearizing the time-τ map. We know that algebraically this linearization is given by Equation 2.3, however, calculating the spatial derivative of the time-τ map is a non-obvious task. In the next two sections, we will use our intuition about the dynamics of time-τ flow to derive an approximation for how perturbations evolve under the time-τ map. In Section 2.4, we will show that this approximation, called the variational equation, is equivalent to the linearization given by Equation 2.3.

2.2 The Variational Equation

From the previous section, we see that the linearization of the flow-kick map is equivalent to the linearization of the time-τ map. Thus to classify the stability of flow-kick equilibria, we must classify the linear approximation of how perturbations from the equilibrium trajectory evolve under the dynamics of time-τ flow. To derive this linear approximation, we can use our intuition about the cumulative dynamics of the vector field along the time-τ flow. Our goal in this section is to derive the variational equation, a tool in dynamical systems used to describe how perturbations spatially evolve through a vector field. In Section 2.4, we will show that the variational equation is the linear approximation of the time-τ map.

Since the goal is to uncover how the dynamics of the vector field evolve solutions relative to the equilibrium trajectory, it seems reasonable to linearize the local dynamics about each point on equilibrium trajectory. Recall from Section 1.2, that the dynamics of the vector field are given by

$$\frac{dX}{dt} = F(X) \tag{2.4}$$

By the same process we used in Section 2.1, we can find an instantaneous local linearization of Equation 2.4 about each point on the solution curve $X(t) = \phi(t, X^*)$.

Since we want to consider the evolution of perturbations from X^*, let $Y(t)$ be a solution of Equation 2.4 with initial condition close to X^*. Let $U(t)$ be the perturbation of $Y(t)$ from $X(t) = \phi(t, X^*)$. So $Y(t) = X(t) + U(t)$ and at any instance $t = \alpha$ we can write:

$$\begin{aligned} \frac{dY}{dt}\Big|_{t=\alpha} &= \frac{d}{dt}\left[X + U\right]\Big|_{t=\alpha} \\ &= \frac{dX}{dt}\Big|_{t=\alpha} + \frac{dU}{dt}\Big|_{t=\alpha} \end{aligned} \tag{2.5}$$

by the linearity of the time derivative operator.

We can also say

$$\begin{aligned} \frac{dY}{dt}\Big|_{t=\alpha} &= \frac{d}{dt}\left[X + U\right]\Big|_{t=\alpha} \\ &= F(X(\alpha)) + U(\alpha)) \\ &\approx F(X(\alpha)) + D\left[F(X(\alpha))\right]U(\alpha) \end{aligned} \tag{2.6}$$

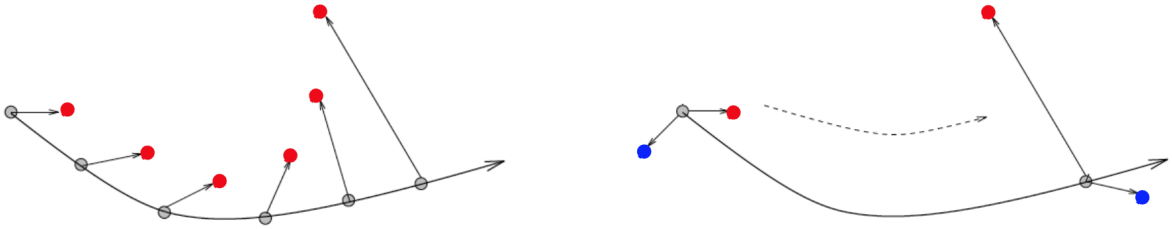

Figure 2.2: (Adapted from Bradley [3].) We think of each point on the equilibrium trajectory contributing something towards the evolution of the perturbation (the red ball). We string together these contributions to get the cumulative effect on the right.

We can now combine 2.5 and 2.6

$$\begin{aligned} \frac{dX}{dt}\Big|_{t=\alpha} + \frac{dU}{dt}\Big|_{t=\alpha} &\approx F(X(\alpha)) + D\left[F(X(\alpha))\right]U(\alpha) \\ \implies \frac{dU}{dt}\Big|_{t=\alpha} &\approx D\left[F(X(\alpha))\right]U(\alpha) \end{aligned} \tag{2.7}$$

This is helpful but we want to know how to approximate the *cumulative* effect of the vector field all along the equilibrium trajectory, not just at one point. Intuitively, we can do this by "stringing along" each of these point-wise approximations (see Figure 2.2). At each moment $t = \alpha$, we approximate $\frac{dU}{dt}\big|_{t=\alpha} = D\left[F(\phi(\alpha, X^*))\right](U(\alpha))$. This yields a differential equation known as the variational equation, defined below.

Definition 2.3. *Given a vector field $F \in C^1$, a flow-kick equilibrium X^*, and the flow $\phi(t, X^*)$, the* **variational equation** *of F about $\phi(t, X^*)$ is given by*

$$\frac{dU}{dt} = D\left[F(\phi(t, X^*))\right] \cdot (U)$$

where $D\left[F(\phi(t, X^*))\right]$ is the spatial derivative of F evaluated at $\phi(t, X^*)$.

The concept of the variational equation is visualized in Figure 2.3. At each point along the equilibrium trajectory, we can linearly approximate the local behavior determined by the differential equation $\frac{dX}{dt} = F(X)$. We imagine that nearby solutions evolve instantaneously according to each of these approximations before moving on to the next.

Just like we have the *flow* and the *time-τ map* for the ODE generated by vector field F (Equation 2.4), we also have the *variational flow* and the *variational time-τ map*.

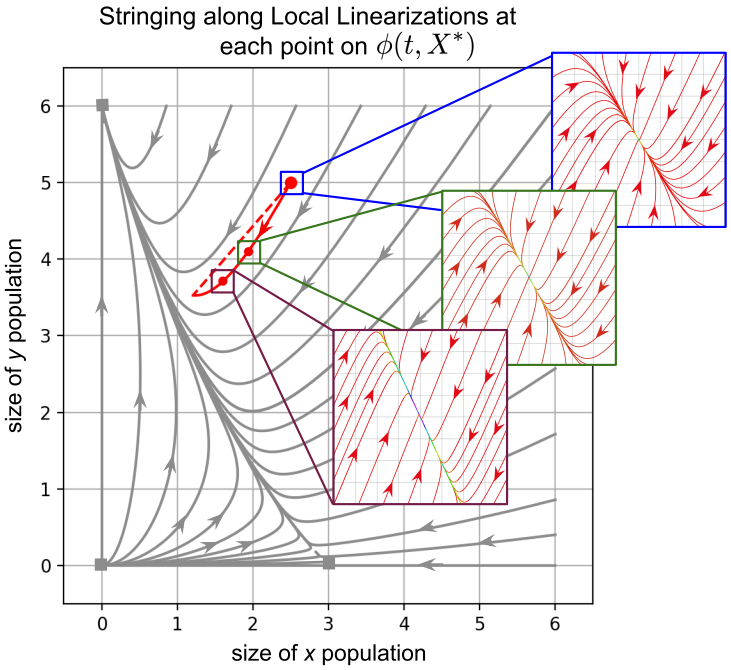

Figure 2.3: The variational equation is obtained by stringing along the instantaneous linear approximation of F about a point on the equilibrium trajectory. The figure shows the instantaneous linear approximation for three points on the equilibrium trajectory. Each is asymptotically attracting with a slightly different speed (indicated by the color gradient) and direction. As time moves in the variational equation, perturbations can be imagined to hop from one linear approximation to another down the equilibrium trajectory, at each moment behavior according to the corresponding linearization.

Definition 2.4. *The* **variational flow** $U(t, U_0)$ *generated by* (F, X^*) *is the solution to the variational equation along* $\phi(t, X^*)$ *with initial perturbation* $U_0 \in \mathbb{R}^n$.

The **variational time-τ map** *is the time-τ map of the variational equation along* $\phi(t, X^*)$. *Using our previous notation:*

$$U_\tau : U_0 \mapsto U(\tau, U_0)$$

where $U(\tau, U_0)$ *is the value of the variational flow with initial perturbation* U_0 *at time* τ.

The goal of this section was to construct a way of approximating the evolution of a perturbation from the equilibrium after one iteration of flow (ie. approximating U_{n+1}

from U_n). The result was a construction of the variational equation which approximates the instantaneous rate of change of perturbations. The variational time-τ map is thus an approximation of the cumulative effect of these dynamics in perturbation space. In the next section, we will look at some properties of the variational equation, and in Section 2.3 we rigorously state the relationship between the variational equation and the linearization of the flow-kick map.

2.3 Properties of the Variational Equation

When $F \in C^1$, the variational equation along a solution to Equation 2.4 is a *continuous, linear, non-autonomous differential equation.* The variational equation is linear because each component of the derivative is linear with respect to the state variables. It is non-autonomous because the derivative depends not only on the current location in state space but also on the current time. The continuity of the variational equation is inherited from the fact that $F \in C^1$.

Continuous linear, non-autonomous differential equations have nice, generally well-understood properties [**?**] which creates a helpful framework from which to start analysing the variational equation. In particular, unique solutions exist for all time by the basic existence and uniqueness theorem for ODEs [5], and we have the following two nice lemmas:

Lemma 2.5. *Given (F, X^*), consider the variational equation along $\phi(t, X^*)$ corresponding to vector field F. Let $U(t, U_0)$ be the solution to the variational equation. $U(t, U_0)$ can be expressed:*

$$U(t, U_0) = U_0 e^{\int_0^t D[F(\phi(s,X^*))]ds} \tag{2.8}$$

Proof. Let's verify the statement by differentiating the expression:

$$\frac{d}{dt}\left[U(t, U_0)\right] = \frac{d}{dt}\left[U_0 e^{\int_0^t D[F(\phi(s,X^*))]ds}\right] = U_0 \frac{d}{dt}\left[\int_0^t D\left[F(\phi(s, X^*)\right]\right] e^{\int_0^t D[F(\phi(s,X^*))]ds}$$

Since $F \in C^1$, $D\left[F(\phi(s, X^*))\right]$ is continuous, and we can apply the fundamental theorem of calculus:

$$\frac{d}{dt}\left[U(t, U_0)\right] = U_0 D\left[F(\phi(t, X^*)\right] e^{\int_0^t D[F(\phi(s,X^*))]ds} = D\left[F(\phi(t, X^*)\right] U(t, U_0)$$

Thus the expression in equation 2.8 does satisfy the variational equation. It is, in fact a solution curve. □

Lemma 2.6. *The time-τ variational map is a linear transformation.*

Proof. To show that U_τ is linear, we must show additivity and scalablity.

Suppose $Z_0 = aX_0 + bY_0$. By the basic existence and uniqueness theorem [5], we know that $U(t, Z_0)$, $U(t, aX_0)$, and $U(t, aY_0)$ exist and are unique. By definition, $aU(0, X_0) + bU(0, Y_0) = aX_0 + bY_0$. Also

$$\begin{aligned}\frac{d}{dt}\left[aU(t, X_0) + bU(t, Y_0)\right] &= a\frac{d}{dt}\left[U(t, X_0)\right] + b\frac{d}{dt}\left[U(t, Y_0)\right] \\ &= aD\left[F(\phi(t, X^*))\right]U(t, X_0) + bD\left[F(\phi(t, X^*))\right]U(t, Y_0) \\ &= D\left[F(\phi(t, X^*))\right](aU(t, X_0) + bU(t, Y_0))\end{aligned}$$

Thus $aU(t, X_0) + bU(t, Y_0)$ is a solution to the variational equation that goes through $aX_0 + bY_0 = Z_0$. This means that $aU(t, X_0) + bU(t, Y_0) = U(t, Z_0)$ and $U_\tau(X_0) + U_\tau(Y_0) = U_\tau(Z_0)$. □

Another aspect of the variational equation that to address is the way that it operates in perturbation space. This means that while the flow-kick trajectories and orbits take place in state space, the dynamics described by the variational equation happen in a space that is related but not equivalent to state space. To clarify this relationship, we define the variational origin:

Definition 2.7. *Given the variational equation of F about $\phi(t, X^*)$, the* **variational origin** *is the origin of the tangent perturbation space (ie. where $U = \mathbf{0} \in \mathbb{R}^n$). At any moment t in time, the* variational origin *is identified with the point $\phi(t, X^*)$ in state space.*

Since at each moment t the variational origin is identified with $\phi(t, X^*)$ on the equilibrium trajectory, we can similarly identify each perturbation U in the variational system with a point $X = \phi(t, X^*) + U$ in state space. In the next section we formalize the relationship between the dynamics in perturbation space defined by the variational equation and the dynamics in state space defined by the flow generated by $\frac{dX}{dt} = F(X)$.

2.4 Linearization via the Variational Equation

Now that we have established the properties of the variational equation, we have the language required to state that the variational equation does what it was constructed to do: it linearly approximates the behavior of perturbations under the dynamics of the system $\frac{dX}{dt} = F(X)$.

For clarity, note that in the following proposition, we use X_n rather than X_0 to denote the initial condition since, in the context of our flow-kick systems, the flow trajectories which we are linearizing start with points on the flow-kick orbit $\{X_n\}$.

Proposition 2.8. (Adapted from Hirsch, Smale, & Devaney) *Given (F, X^*), let $\phi(t, X_n)$ be the flow generated by $\frac{dX}{dt} = F(X)$ through $X_n = X^* + U_n$ and let $U(t, U_n)$ be the solution to the variational equation along $\phi(t, X^*)$ through $U_n \in \mathbb{R}^n$. Then*

$$\lim_{U_n \to \mathbf{0}} \frac{||\phi(t, X_n) - (\phi(t, X^*) + U(t, U_n))||}{||U_n||}$$

converges uniformly to zero for $t \in [0, \tau]$.

Proof. See Hirsch, Smale, & Devaney Chapter 17 [5]. □

Proposition 2.8 formally justifies our intuition: $\phi(t, X^* + U_n) \approx \phi(t, X^*) + U(t, U_n)$. From this result, we now have an even better way of approximating U_{n+1} given U_n.

Corollary 2.9. *If U_n is sufficiently small, than $U_\tau(U_n)$ is a good approximation for U_{n+1}.*

Proof.

$$\begin{aligned} & \phi(t, X^*) + U(t, U_n) \approx \phi(t, X_n) && \text{by Proposition 2.8} \\ \implies & \phi_\tau(X^*) + U_\tau(U_n) \approx \phi_\tau(X_n) \\ \implies & U_\tau(U_n) \approx \phi_\tau(X_n) - \phi_\tau(X^*) = U_{n+1} && \text{by Lemma 2.2} \end{aligned} \tag{2.9}$$

□

Now we have two approximations of U_{n+1}, one from the linearization approach (Equation 2.3) and the other from the variational approach (Equation 2.9). The following result shows that these two approximations are identical!

Theorem 2.10. (Adapted from Hirsch, Smale, & Devaney) *Given (F, τ, X^*), let $D[\phi_\tau(X^*)]$ be the spatial derivative of the time-τ map generated by $\frac{dX}{dt} = F(X)$ and evaluated at the flow-kick equilibrium X^*. Let U_τ be the variational time-τ map associated with the variational equation along $\phi(t, X^*)$. Then for any perturbation U_n from the equilibrium*

$$D[\phi_\tau(X^*)](U_n) = U_\tau(U_n)$$

Proof. (Adapted from Hirsch, Smale, & Devaney)

First, note that the spatial derivative applied to any vector is the directional derivative in the direction of that vector scaled by the norm. By linearity, we can assume without loss of generality that $||U_n|| = 1$. Thus $D[\phi_\tau(X^*)](U_n)$ is the directional derivative of ϕ_τ in the direction of U_n evaluated at X^*.

We can write this directional derivative using the limit definition of the derivative:

$$D[\phi_\tau(X^*)](U_n) = \lim_{h\to 0} \frac{\phi_\tau(X^* + hU_n) - \phi_\tau(X^*)}{h} \tag{2.10}$$

By Proposition 2.8,

$$\lim_{h\to 0} \frac{||\phi_\tau(X^* + hU_n) - (\phi_\tau(X^*) - U_\tau(hU_n))\,||}{h}$$

converges to zero uniformly. This is equivalent to saying that

$$\lim_{h\to 0} \frac{(\phi_\tau(X^*) - U_\tau(hU_n))}{h} = \lim_{h\to 0} \frac{\phi_\tau(X^* + hU_n)}{h}$$

Thus we can simplify the right-hand side of 2.10:

$$\begin{aligned} D[\phi_\tau(X^*)](U_n) &= \lim_{h\to 0} \frac{\phi_\tau(X^*) + U_\tau(hU_n) - \phi_\tau(X^*)}{h} \\ &= \lim_{h\to 0} \frac{U_\tau(hU_n)}{h} = \lim_{h\to 0} \frac{hU_\tau(U_n)}{h} && \text{by linearity, Lemma 2.6} \\ &= U_\tau(U_n) \end{aligned}$$

□

Not only does Theorem 2.10 mean that our two approximations are identical, it means that we have a way of calculating the spatial derivative of the time-τ map and, more importantly, we have a way to linearize the flow-kick map $G_{\tau,k}$.

In Chapter 3, we will develop analytic approaches to characterizing the variational equation so as to use this linearization to classify the stability of flow-kick equilibrium. In Chapter 5 we will discuss how numerical techniques can be used to find the stability of the variational time-τ map, and thus the flow-kick equilibrium, for a given flow-kick system with equilibrium X^*.

Chapter 3

Reactivity and the Variational Equation

3.1 Stability of Autonomous, Linear Systems

In Chapter 2, we established that the variational time-τ map is the linearization of the flow-kick map around the flow-kick equilibrium (Theorem 2.10). We will now turn to how to classify the stability of the variational time-τ map and the variational equation in general. In this section we will build our intuition by reviewing known techniques for stability classification of both continuous and discrete autonomous, linear approximations.

Before we dig into current classification techniques, let's establish which systems we are working with. In this chapter we will primarily focus on two-dimensional systems with the knowledge that many of the techniques and results presented in two dimensions can be generalized to higher dimensions. We will work with both discrete and continuous dynamical systems. Since we are thinking about how to classify linearizations, we will be considering autonomous, linear dynamical systems. A discrete autonomous, linear system is given by a difference equation of the form:

$$X_{n+1} = AX_n \tag{3.1}$$

where A is a real 2×2 matrix. Similarly a continuous autonomous, linear system is given by a differential equation of the form:

$$\frac{dX}{dt} = AX \tag{3.2}$$

where A is again a real 2×2 matrix.

The stability of an autonomous linear system is most often determined by the eigenvalues of the corresponding matrix A. The eigenvalues of A, denoted λ_1 and λ_2, solve the eigenvalue problem $AV = \lambda V$ for eigenvectors $V \in \mathbb{R}^2$. To fix our ideas, consider the case when A has a real eigenvalue λ. If we pick an eigenvector V_0 as the initial value through which to solve either the discrete system (Equation 3.1) or the continuous system (Equation 3.2), we get an eigenvector solution. In the discrete case, an eigenvector solution can be expressed as:

$$V_n = \lambda^n V_0 \qquad \text{with} \qquad AV_0 = \lambda V_0 \tag{3.3}$$

An eigenvector solution in a continuous system can be expressed as:

$$V(t) = V_0 e^{\lambda t} \qquad \text{with} \qquad AV_0 = \lambda V_0 \tag{3.4}$$

A nice property of autonomous, linear systems is that their general solutions can always be expressed by linear combinations of the eigenvector solutions. Thus, besides being well-behaved special cases, eigenvector solutions can tell us a lot about the general classification of their corresponding linear systems.

With this in mind, let's continue to analyze the properties of eigenvector solutions. From Equations 3.3 and 3.4 we observe that eigenvalue solutions lie on straight lines are invariant under the dynamics of their corresponding linear systems. We often talk about these invariant sets as *eigenlines* under which the dynamics of the linear system can be reduced to one-dimension. In that one-dimension the dynamics consist simply of movement toward or away from the origin (or possibly a line of fixed points). As can be seen in Equations 3.3 and 3.4 the coefficient that the determines this movement is the eigenvalue.

The criteria that determines whether an eigenvalue results in attraction or repulsion along the invariant eigenline differs between continuous and discrete systems. In a discrete system (like the time-τ variational map), the eigenvalue λ describes the proportionality constant for the growth or shrinkage of the vector in its next iteration: $V_{n+1} = \lambda V_n$. Thus $|\lambda| < 1$ results in the eigenvector being scaled down in each iteration (ie. the movement toward the origin). If $|\lambda| > 1$, the eigenvector is being scaled up in each iteration (ie. the movement is away from the origin). If $|\lambda| = 1$, then the eigenvector itself is invariant under the dynamics of the discrete system.

In a continuous system, the eigenvalue λ describes the velocity with which the solution moves along the invariant eigenline in time: $\frac{dV}{dt} = \lambda V$. This means that if $\lambda < 0$, the velocity

is in the opposite direction as the eigenvector and the solution moves toward the origin in time. If $\lambda > 0$, velocity is in the same direction as the eigenvector and the solution moves away from the origin in time. If $\lambda = 0$, then the eigenvector is actually an equilibrium of the system since it always has zero velocity.

In the case when $\lambda_1, \lambda_2 \in \mathbb{C}$, they form a complex conjugate pair, and the criteria for continuous systems applies to the real part $re(\lambda_i)$ of the eigenvalues while the criteria for discrete systems applies to the modulus $|\lambda_i|$ of the complex eigenvalue. For more information about how to interpret complex eigenvalues and eigenvectors, see [5].

Since the general solutions to autonomous linear systems in higher dimensions involve linearly combining eigenvector solutions, we apply the criteria discussed above to multiple eigenvalues simultaneously. If all eigenvalues show attraction, then the equilibrium is attracting. If all eigenvalues show repulsion, then the equilibrium is repelling. If some eigenvalues show attraction and some repulsion, then the equilibrium is a saddle. Note that for the purposes of this chapter, we will not state the special cases where one or more of the eigenvalues shows neither attracting nor repelling. For a broader overview of this classification, see [5].

This eigenvalue method of characterizing the stability of equilibria is outlined for the general cases in Table 3.1.

	Criteria	**Classification**
Discrete system		
	$\lvert\lambda_1\rvert \leq \lvert\lambda_2\rvert < 1$	stable, attracting, sink
	$\lvert\lambda_1\rvert < 1 < \lvert\lambda_2\rvert$	unstable, saddle
	$1 < \lvert\lambda_1\rvert \leq \lvert\lambda_2\rvert$	unstable, repelling, source
Continuous system		
	$re(\lambda_1) \leq re(\lambda_2) < 0$	stable, attracting, sink
	$re(\lambda_1) < 0 < re(\lambda_2)$	unstable, saddle
	$0 < re(\lambda_1) \leq re(\lambda_2)$	unstable, repelling, source

Table 3.1: A summary of the eigenvalue criteria for stability classification in both discrete and continuous systems.

We now have a method for classifying both discrete and continuous autonomous linear dynamical systems based on their eigenvalues. Note that by Lemma 2.6, the discrete system

generated by iterating the variational time-τ map is itself a discrete autonomous, linear system. If we had a matrix representation of U_τ, we could classify the stability of our flow-kick equilibrium based on the criteria given in Table 3.1. Though we don't have a general matrix representation of U_τ, we can generate it computationally for specific examples by simply simulating the variational equation for two linearly independent initial conditions. We will briefly discuss uses for this numerical approach used in Chapter 5.

In the interest of understanding the dynamics of the variational equation and developing an analytic technique for classifying the variational time-τ map, the next section will address how to generalize the techniques of eigenvalue analysis outlined in this section to the variational equation.

3.2 Analyzing the Variational Equation

Recall that our goal is to classify the stability of an equilibrium of a flow-kick system by analyzing the dynamics of the associated variational equation along the equilibrium trajectory of the flow-kick system.

Notation 3.1. To establish our notation, consider a flow-kick map $G_{\tau,k}$ with an equilibrium point at X^*. In the notation of Definition 1.2, $G_{\tau,k}$ is generated by a triple $(F, \tau, k) \in C^1(\mathbb{R}^n) \times \mathbb{R} \times \mathbb{R}^n$. However, as we have seen in Lemma 2.2, the kick vector, k, plays no role in determining the linearization of $G_{\tau,k}$ at X^*. Moreover, from Lemma 1.9, we know that given any triple $(F, \tau, X^*) \in C^1(\mathbb{R}^n) \times \mathbb{R} \times \mathbb{R}^n$, there is a unique kick vector k such that X^* is an equilibrium of $G_{\tau,k}$. Thus, we can use the triple (F, τ, X^*) to define a flow-kick map $G_{\tau,k}$ with equilibrium point at X^*. Similarly given a vector field $F \in C^1(\mathbb{R}^n)$, we can use the pair (τ, X^*) to define the flow-kick map $G_{\tau,k}$.

Focusing on flow-kick systems that all have the same underlying vector field F is very useful to many applications. In a decision support scenario, for example, we would most likely have a fixed model for the underlying ecological system in the form of a vector field F. We would then be interested in finding the set of (τ, X^*) pairs for which X^* is an attracting flow-kick equilibrium that represents a healthy ecological system.

Notice that for any choice of (F, τ, X^*), the stability classification of X^* is based on how the instantaneous linearizations along the equilibrium trajectory contribute to the dynamics

of the variational time-τ map. Since any point in state space could be on the equilibrium trajectory for some pair (τ, X^*), we will perform an eigenvalue analysis of the instantaneous linearization of F about every point in state space.

To begin this generalized eigenvalue analysis of the linearization of F at any X in state space, let's walk through the symbolic computations that are required. Note that, as in the previous section, we will assume that our systems are two-dimensional, knowing that most results generalize to higher dimensions. Given a vector field $F \in C^1(\mathbb{R}^2)$, the autonomous linear approximation around an arbitrary point $X \in \mathbb{R}^2$ is given by:

$$\frac{dU}{dt} = D[F(X)]U \tag{3.5}$$

The eigenvalues of $D[F(X)]$ can be found by solving the characteristic polynomial:

$$0 = \lambda^2 - \mathrm{tr}\left(D[F(X)]\right)\lambda + \det\left(D[F(X)]\right) \tag{3.6}$$

where $tr\left(D[F(X)]\right)$ represents the trace and $\det\left(D[F(X)]\right)$ represents the determinant of the matrix $D[F(x)]$.

Up to this point we have done three sets of symbolic computations: $D[F(X)]$, $\mathrm{tr}\left(D[F(X)]\right)$, and $\det\left(D[F(X)]\right)$. Although we could perform a fourth symbolic computation to solve the characteristic polynomial, this is a more computationally expensive calculation. Instead, we note that for stability classification, we are concerned with which criteria the eigenvalues meet rather than the actual values of λ_1 and λ_2. Fortunately, we can create an equivalent set of criteria based on the coefficients of the characteristic polynomial (Equation 3.6). These new criteria are given for continuous systems in Lemma 3.2 and visually summarized in Figure 3.2.

Lemma 3.2. *(Trace-Determinant Criteria) Consider a two-dimensional linear differential equation* $\frac{dX}{dt} = AX$.

1. *If* $\det(A) < 0$, *then* $re(\lambda_1) < 0 < re(\lambda_2)$ *and the equilibrium is a saddle.*
2. *If* $\det(A) > 0$ *and* $tr(A) < 0$, *then* $re(\lambda_1) \leq re(\lambda_2) < 0$ *and the equilibrium is an attractor.*
3. *If* $\det(A) > 0$ *and* $tr(A) > 0$, *then* $0 < re(\lambda_1) \leq re(\lambda_2)$ *and the equilibrium is a repeller.*

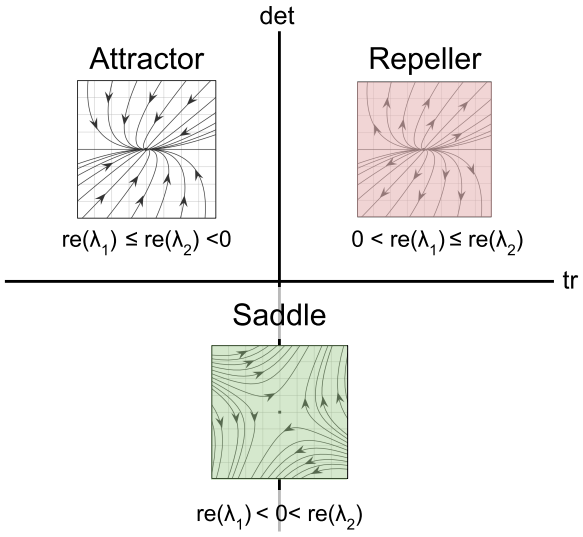

Figure 3.1: Since the trace-determinant criteria are based on when trace and determinant are positive or negative, we can characterize the general classifications as belonging to one of the regions of the trace determinant plane. For example, in the first quadrant of the trace-determinant plane we have repellers since it is here where both the trace and the determinant are positive.

With expressions for the trace and determinant of $D[F(X)]$, the criteria in Lemma 3.2 provides systems of inequalities which define regions of state space in which the instantaneous linearization around every point has the same classification. These regions are defined below:

These regions are outlined in Definition 3.3. Example 3.4 shows the symbolic calculations needed to generate these regions for Figure 3.2.

Definition 3.3. *Given a vector field $F \in C^1(\mathbb{R}^2)$,*

*The **attracting region** $\mathcal{A}$ of state space is the set of all points $X \in \mathbb{R}^2$ such that the linearization of F about X (Equation 3.5) has an attracting equilibrium.*

*The **saddle region** $\mathcal{S}$ of state space is the set of all points $X \in \mathbb{R}^2$ such that the linearization of F about X (Equation 3.5) has a saddle equilibrium.*

*The **repelling region** $\mathcal{R}$ of state space is the set of all points $X \in \mathbb{R}^2$ such that the linearization of F about X (Equation 3.5) has a repelling equilibrium.*

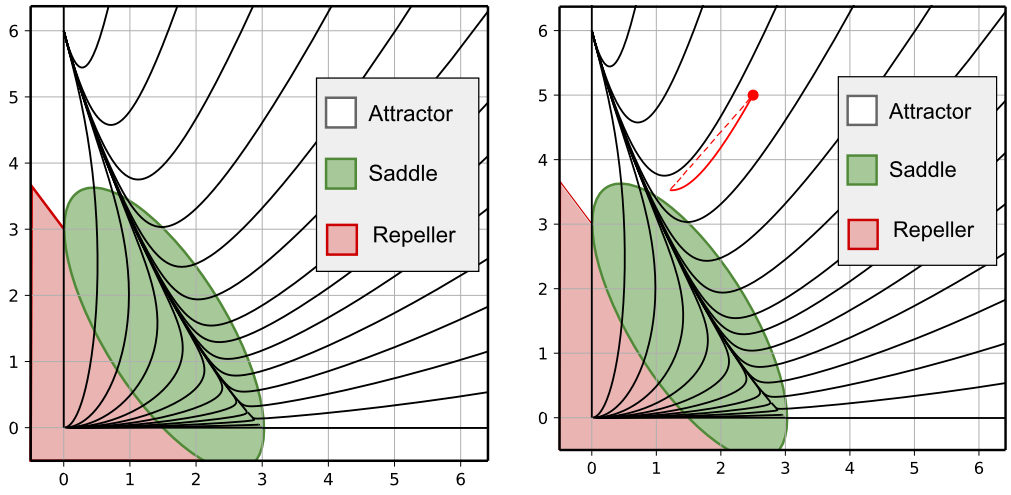

Figure 3.2: (a) The linearization of F about each point in the state space can be classified using the trace-determinant criteria. Depicted is state space broken into classification regions colored to correspond with Figure 3.2. (b) The equilibrium trajectory of interest for this flow-kick system is composed of points in state space that are each contained in the attracting region. We can imagine the linearized dynamics at each point, characterized by their asymptotic classification, accumulating in time.

Example 3.4 shows the symbolic calculations needed to generate the regions given in Definition 3.3. Figure 3.2 visualizes the classification regions generated by the system in Example 3.4.

Example 3.4. Consider the family of flow-kick systems associated with the two-dimensional ODE:

$$\frac{dX}{dt} = F(x,y) = \begin{pmatrix} f(x,y) \\ g(x,y) \end{pmatrix} = \begin{pmatrix} 0.09x\left(1 - \dfrac{x-y}{3}\right) \\ 0.18y\left(1 - \dfrac{y-2x}{6}\right) \end{pmatrix}$$

We need to find an expression for the instantaneous linearization of the ODE at any

point in state space. We know this is done by computing the Jacobian matrix of $F(x, y)$.

$$D[F(x,y)] = \begin{pmatrix} f_x(x,y) & f_y(x,y) \\ g_x(x,y) & g_y(x,y) \end{pmatrix} = \begin{pmatrix} 0.09 - 0.06x - 0.03y & -0.03x \\ -0.06y & 0.18 - 0.06x - 0.06y \end{pmatrix}$$

By the trace-determinant criteria (Lemma 3.2), all we must do now to classify the asymptotic stability of each instantaneous linearization is to calculate the trace and determinant of $D[F]$.

$$\begin{aligned} \text{tr}(D[F(x,y)]) &= (0.09 - 0.06x - 0.03y) + (0.18 - 0.06x - 0.06y) \\ &= 0.27 - 0.12x - 0.09y \\ \det(D[F(x,y)]) &= (0.09 - 0.06x - 0.03y)(0.18 - 0.06x - 0.06y) - (-0.03x)(-0.06y) \\ &= 0.0036(4.5 - 4.5x + 1.x^2 - 3.y + 1.xy + 0.5y^2) \end{aligned}$$

Now we have an expression for $\text{tr}(D[F])$ and $\det(D[F])$ in terms of (x, y) we can use the trace-determinant criteria to find and plot the attracting, repelling, and saddle regions of state space. To fix our understanding, let's follow this procedure for the attracting region.

For (x, y) to be in the attracting region, the instantaneous linear approximation of F about that point must be attracting. That means that we need

$$\begin{aligned} \det(D[F(x,y)]) &= 0.0036(4.5 - 4.5x + 1.x^2 - 3.y + 1.xy + 0.5y^2) > 0 \\ \text{tr}(D[F(x,y)]) &= 0.27 - 0.12x - 0.09y < 0 \end{aligned}$$

The region where both of these inequalities hold is represented by the white region of state space in Figure 3.2. Similarly the repelling and saddle regions are represented by the red and green regions respectively.

Though these regions refer to the classification of the instantaneous linearization of F, we can use them to build intuition about the dynamical behavior of a variational equation. Remember that for any $F \in C^1(\mathbb{R}^2)$, every point in state space is of an equilibrium trajectory for some pair (τ, X^*). If a point X is on the equilibrium trajectory and is in the attracting region, then we might hypothesize that its contribution to the cumulative dynamics of the variational equation is attraction. Similarly, if the point was in the saddle or repelling region we might hypothesize that it contributes saddle or repelling behavior respectively.

In other words, we can think about all the points on the equilibrium trajectory, and

which stability region they are contained in, to try and get a moment-by-moment classification of the dynamical behavior of the variational equation. In Conjecture 3.5, we consider the question: Can we apply the logic of "stringing along" stability classifications in the same way that we did linearized dynamics to construct the variational equation?

Conjecture 3.5. *Given a triple (F, τ, X^*) and the associated flow-kick map $G_{\tau,k}$:*

Let $\mathcal{A}$ denote the attracting region of state space. If, $\forall t \in [0, \tau]$, $\phi(t, X^*) \in \mathcal{A}$, then X^* is an attracting flow-kick equilibrium.

Let $\mathcal{R}$ denote the repelling region of state space. If, $\forall t \in [0, \tau]$, $\phi(t, X^*) \in \mathcal{R}$, then X^* is a repelling flow-kick equilibrium.

It would seem that if an equilibrium trajectory is entirely contained within a particular classification region, then the accumulation of those dynamics (ie. the variational time-τ map) should have that same stability classification.

We seem to have a good intuitive basis for this conjecture being true: we used the method of stringing along dynamics in order to generate the variational equation and we ended up with a formal linearization of the flow-kick map. It might seem that if an equilibrium trajectory is entirely contained within a particular classification region, then the accumulation of those dynamics (ie. the variational time-τ map) should have that same stability classification. We must recognize, however, that the case of stringing along classifications is different than stringing along linearized dynamics. Significantly, an eigenvalue classification describes the *asymptotic* behavior of the system while the contribution of linearized dynamics along the equilibrium trajectory is implicitly of an instantaneous and transient nature. While it is true for each instantaneous linearization all solutions end up conforming to the behavior described by the eigenvalues, Example 3.6 will show that it is possible for the transient behavior of the system (and thus its contribution to the variational equation) to differ from its asymptotic classification.

Example 3.6. To illustrate how asymptotic and transient behavior can differ from one another, consider the system:

$$\frac{dX}{dt} = AX = \begin{pmatrix} -1 & 10 \\ 0 & -3 \end{pmatrix} X \tag{3.7}$$

The eigenvalues of A are $\lambda_1 = -1$ and $\lambda_2 = -3$ and we can see from Figure 3.2 that the solution is being attracted to the origin. However for some solutions there is a short period of time (highlighted in red) during which the solution moves *away* from the origin.

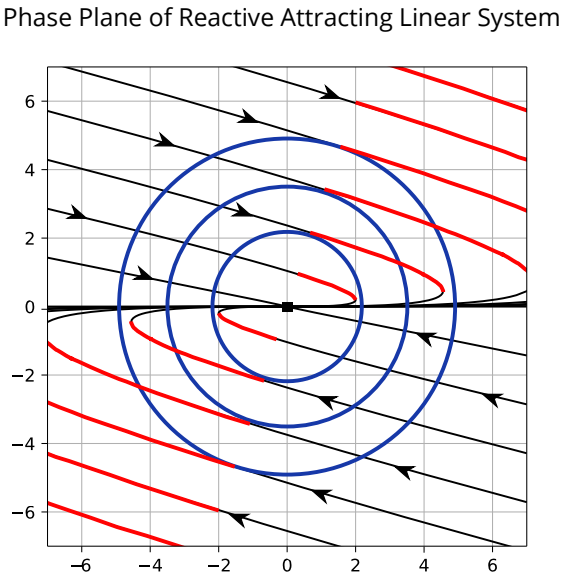

Figure 3.3: Solutions to this linear system $\frac{dX}{dt} = \begin{pmatrix} -1 & 10 \\ 0 & -3 \end{pmatrix} X$ are attracted to the origin, but during their approach they move further away from the origin before being asymptotically attracted. These periods of temporary movement away from the origin are highlighted in red. The blue concentric circles provide landmarks for recognizing when a solution's approach switches between movement away from the origin and movement toward.

The difference between asymptotic and transient behavior is significant because the systems we are classifying operate not as stand-alone linear systems but as *instantaneous* linear approximations of underlying flow dynamics. We are primarily concerned with the instantaneous contribution these approximations make to the cumulative behavior of the variational equation. Though it is possible that the asymptotic behavior of a system could describe its instantaneous contribution to the variational equation, we see from Example 3.6 that we can't assume it will.

Based on Example 3.6, we can imagine a scenario in which at each moment $t \in [0, \tau]$, the perturbation $U(t, U_0)$ is driven further away from the variational origin by the instantaneous contribution of the linear approximation at $\phi(t, X^*)$. In this scenario, one iteration of the

variational time-τ map would have a repelling effect even if the trajectory about which we are constructing the variational equation is contained entirely withing the attracting region. In Chapter **??**, we construct an example of a non-autonomous linear differential equation (though not a variational equation) where this happens for many choices of $\tau \in \mathbb{R}$.

It is these conceived scenarios that make our conjecture non-obvious. As we continue to explore whether or not we can prove or disprove our conjecture, we must consider the following questions: To what degree can transient behavior differ from the asymptotic behavior as described by the eigenvalues? If they do differ, which behavior dominates the system's contribution to variational equation? Under what circumstances can we be confident that the asymptotic classification *does* describe the system's contribution to the variational equation?

These questions are addressed in the next two section of Chapter 3.

3.3 Reactivity and Transient Behavior

To characterize transient behavior and address the effect it has in the cumulative dynamics of the variational equation, we must introduce some new language. In particular we want a way to describe the "worst case" transient behavior. Reactivity is a property of linear systems that describes the maximum instantaneous amplification of solutions.

Definition 3.7. *The* **reactivity** *of an autonomous, linear system $\frac{dX}{dt} = AX$ is the maximum radial velocity of that system on the unit circle:*

$$\rho(A) = \max_{||X_0||=1} \left\{ \frac{d||X||}{dt}\Big|_{t=0} \right\} \tag{3.8}$$

Note that because the system is linear, the reactivity ρ gives not just the maximum amplification of points on the unit circle but also the maximum normalized amplification for all points in state space.

A key feature of reactivity is that it provides an upper bound for transient growth behavior. It says, "The reactivity ρ measures the fastest any solution could be moving away from the origin at any instant in time."

Having an upper bound for transient growth behavior is extremely useful when determining whether an asymptotically attracting linear system ever exhibits transient repelling

behavior. If the reactivity is negative, then solutions to the system can only ever be moving toward the attracting equilibrium. If the reactivity is positive, then there are some solutions that move away from the origin for some period of time before asymptotically being attracted back to the origin (see Figure 3.3).

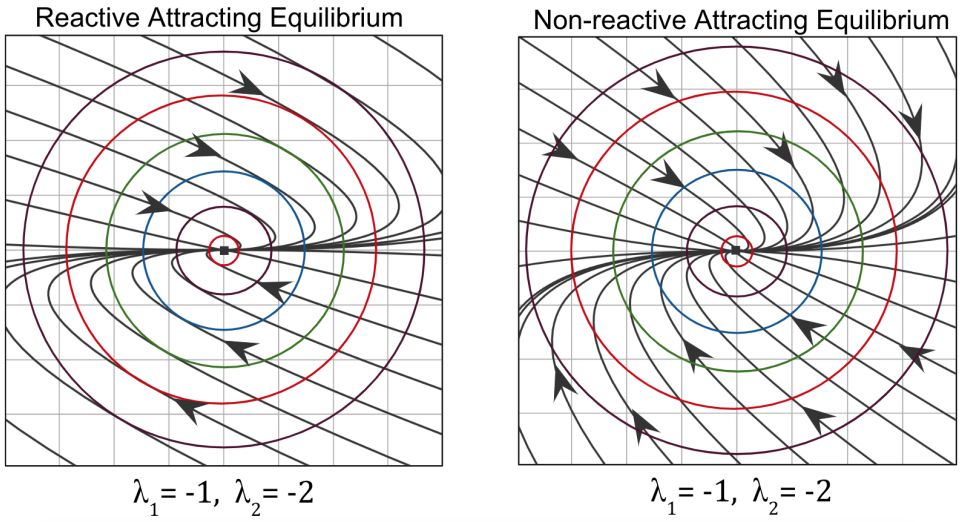

Figure 3.4: Two linear systems can have the same eigenvalues without showing the same transient behavior. The phase portrait on the left is given by $\frac{dX}{dt} = \begin{pmatrix} -1 & 10 \\ 0 & -2 \end{pmatrix} X$ and is reactive. The phase portrait on the right is given by $\frac{dX}{dt} = \begin{pmatrix} -1 & 2 \\ 0 & -2 \end{pmatrix} X$ and is non-reactive.

Definition 3.8. *An autonomous linear system* $\frac{dX}{dt} = AX$ *is* **reactive** *if its reactivity is positive. It is* **non-reactive** *if its reactivity is negative.*

Remark 3.9. Let's take a moment to build an intuition for why these systems are called "reactive." Consider graphing a solution's distance from the origin at each point in time (ie. the solutions norm over time). In a system that is not reactive, any perturbation from the origin would just slowly diminish and return the solution to the origin. In a reactive system, solutions "react" to the perturbation before returning to equilibrium. In a sense, the perturbation is like a catalyst in a chemical reaction or a stimulating voltage for a neuron's action potential. See Figure 3.3.

Reactivity gives us the language to discuss one extreme of a system's transient behavior. Fortunately the reactivity is also a value we can calculate symbolically with relative ease as we will see in Theorem 3.11. First, we review the decomposition of a matrix A into its Hermitian

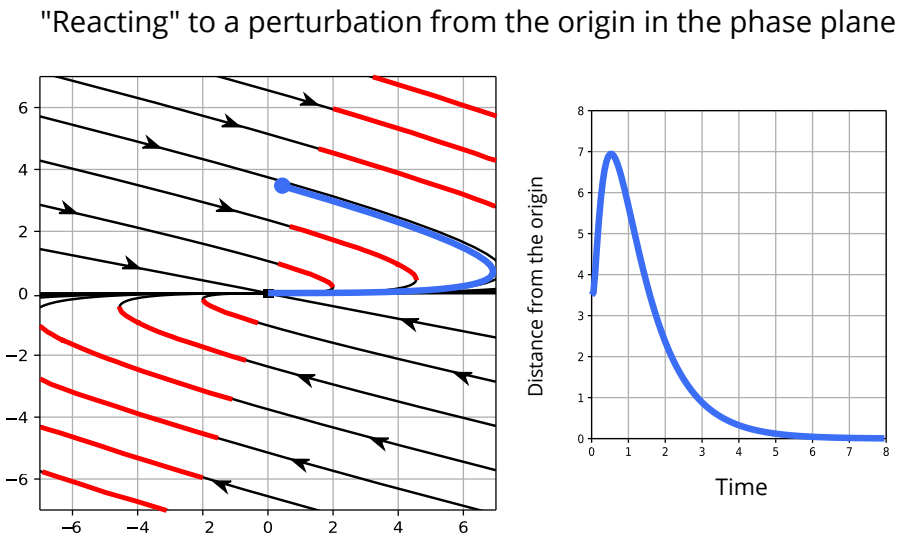

Figure 3.5: In a reactive attracting system perturbations from the origin cause solutions to move further away from the origin before attracting back to it. On the right, we see the the solution's distance from the origin over time. From this perspective, it appears that the solution is "reacting" to being perturbed from the origin.

(symmetric) and antihermitian (skew-symmetric) parts. A definition of this decomposition is given below.

Definition 3.10.

The **Hermitian** *part of a matrix A, also called the* **symmetric** *part of A, is given by:*

$$H(A) = \frac{A + A^T}{2}$$

The **antihermitian** *part of A, also called the* **skew-symmetric** *part of A, is given by:*

$$S(A) = \frac{A - A^T}{2}$$

Notice that $A = H(A) + S(A)$. In Chapter 4, we explore the properties of $H(A)$ and $S(A)$. In particular we will build intuition about which properties of A this decomposition

extracts and how they relate to our present context. For now, we will use $H(A)$ to calculate the reactivity. Note that since $H(A)$ is real and symmetric, all its eigenvalues are real.

Theorem 3.11. *(Adapted from Neubert & Caswell [10]) Consider an autonomous, linear differential equation $\frac{dX}{dt} = AX$. Then the reactivity of the system is given by the largest eigenvalue of the Hermitian part of A:*

$$\rho(A) = \max\{\Lambda(H(A))\} \tag{3.9}$$

where $\Lambda(H(A))$ is the set of eigenvalues of $H(A)$.

Proof. (Adapted from Neubert & Caswell [10])

Recall that the definition of reactivity involves calculating the derivative of the norm of X (ie. $\frac{d||X||}{dt}$). Assuming we are working with the usual Euclidean distance, we can make the following computations: if $||X|| = 1$,

$$\begin{aligned}
\frac{d}{dt}\Big[||X||\Big]_{t=0} &= \frac{d}{dt}\left[\sqrt{X^T X}\right]_{t=0} \\
&= \frac{1}{2}\frac{1}{\sqrt{X_0^T X_0}}\left(X_0^T \frac{dX}{dt}\Big|_{t=0} + \frac{dX^T}{dt}\Big|_{t=0} X_0\right) \\
&= \frac{X_0^T A X_0 + X_0^T A^T X_0}{2} \\
&= \frac{X_0^T (A + A^T) X_0}{2} \\
&= X_0^T H(A) X_0
\end{aligned} \tag{3.10}$$

Note that this last expression 3.10 is the *Rayleigh quotient* of $H(A)$ at X_0. By Rayleigh's Theorem the maximum Rayleigh quotient over all points on the unit circle is the largest eigenvalue of $H(A)$ [6]. We can thus write

$$\rho(A) = \max_{||X_0||=1}\left\{\frac{d||X||}{dt}\Big|_{t=0}\right\} = \max_{||X_0||=1}\left\{X_0^T H(A) X_0\right\} = \max\{\Lambda(H(A))\}$$

□

Theorem 3.11 is significant not only because it offers a way of calculating the the reactivity, but also because it provides a way to characterise the maximum transient growth behavior in a handful of symbolic computations similar to those performed in Section 3.2.

So far we have focused on attracting systems that may exhibit reactivity. We can also conceive of repelling systems that may have transient attracting behavior. In essence this is the same as reactivity but in reverse. Instead of having solutions that are ultimately attracted to the origin but react first, we have solutions that are ultimately repelled from the origin but backtrack towards the origin before heading to infinity. In the following definition, we establish the language of reverse reactivity in order to talk about this type of system.

Definition 3.12. *The* **reverse reactivity** *of an autonomous, linear system is the minimum radial velocity of that system on the unit circle.*

$$\sigma = \min_{||X_0||=1} \left\{ \frac{d||X||}{dt}\Big|_{t=0} \right\} \tag{3.11}$$

A system is **reverse reactive** *if its reverse reactivity is negative. A system is* **reverse non-reactive** *if its reverse reactivity is positive.*

Fortunately, just like the reactivity, reverse reactivity is easy to symbolically calculate:

Theorem 3.13. *Consider an autonomous, linear differential equation* $\frac{dX}{dt} = AX$*. Then the reverse reactivity of the system is given by the smallest eigenvalue of the Hermitian part of* A*:*

$$\sigma(A) = \min\{\Lambda(H(A))\} \tag{3.12}$$

where $\Lambda(H(A))$ *is the set of eigenvalues of* $H(A)$*.*

The proof of Theorem 3.13 follows similarly to the proof of Theorem 3.11. In fact, many of the results for reactivity have a parallel result for reverse reactivity. This is a product of the innate connection between reactivity and reverse reactivity suggested by their names and described formally in Lemma 3.14 and Corollary 3.15.

Lemma 3.14. *The linear system* $\frac{dX}{dt} = AX$ *is reverse reactive if and only if it is reactive in reverse time.*

Proof. First note that $\frac{dX}{dt} = AX$ in reverse time is given by $\frac{dX}{dt} = -AX$. In other words, every time dynamics has been reversed.

Suppose that the linear system $\frac{dX}{dt} = AX$ is reverse reactive. Then we can write:

$$\begin{aligned} & \sigma(A) = \min\{\Lambda(H(A))\} < 0 \\ \iff & -\max\{\Lambda(H(-A))\} < 0 \\ \iff & -\rho(-A) < 0 \\ \iff & \rho(-A) > 0 \end{aligned}$$

The last statement means that $\frac{dX}{dt} = -AX$ is reactive. Thus $\frac{dX}{dt} = AX$ being reverse reactive implies that it is reactive in reverse time and vice versa. □

Corollary 3.15. *The linear system $\frac{dX}{dt} = AX$ is reverse non-reactive if and only if it is non-reactive in reverse time.*

We now have a way to compute and discuss both extremes of transient behavior for general linear non-autonomous differential equations. In particular, we can apply this method for characterizing transient behavior to the instantaneous linearizations of the vector field F that make up the variational equation. This reactivity classification and its use in conjunction with our asymptotic classification (see Definition 3.3 and Figure 3.2) are discussed in the following sections.

3.4 Reactivity Classification of State Space

We will begin this reactivity classification process from the same place we began our asymptotic classification process. Let $F \in C^1(\mathbb{R})$, and consider the instantaneous linearization of F about any point $X \in \mathbb{R}^2$:

$$\frac{dU}{dt} = D[F(X)]U \tag{3.13}$$

Any point $X \in \mathbb{R}^2$ can be on the equilibrium trajectory for some choice of (τ, X^*). Thus for any $X \in \mathbb{R}^2$, Equation 3.13 may be one of the contributing autonomous linear approximations of the variational equation. We have already classified every such linearization based on their asymptotic behavior (as indicated by the eigenvalues of $D[F(X)]$).

In this section, we want to go a step further to measure the range of possible transient behavior in each of these instantaneous linear approximations. Using Theorems 3.11

and 3.13, we can find this range for any point $X \in \mathbb{R}^2$ by characterizing the eigenvalues of $H(D[F(X)])$. In fact, because the classification of reactive/non-reactive and reverse reactive/reverse non-reactive depends only on with the sign of the eigenvalues of $H(D[F(X)])$ and not the values themselves, we can establish trace-determinant criteria for reactivity that will ease the computational cost of characterizing the reactivity $\rho(D[F(X)])$ over all of state space.

Lemma 3.16. *(Trace-determinant criteria for reactivity) Consider a two-dimensional autonomous linear differential equation* $\frac{dX}{dt} = AX$. *Let* $\lambda_1, \lambda_2 \in \mathbb{R}$ *be the eigenvalues of* $H(A)$.

1. *If* $\det(H(A)) < 0$, *then* $\lambda_1 < 0 < \lambda_2$ *and the system is both reactive and reverse reactive.*
2. *If* $\det(H(A)) > 0$ *and* $tr(H(A)) < 0$, *then* $\lambda_1 < \lambda_2 < 0$ *and the system non-reactive and reverse reactive.*
3. *If* $\det(H(A)) > 0$ *and* $tr(H(A)) > 0$, *then* $0 < \lambda_1 < \lambda_2$ *and the system is reactive and reverse non-reactive.*

The proof of Lemma 3.16 follows quickly by applying Lemma 3.2 to the Hermitian part of A and using the calculations presented in Theorems 3.11 and 3.13 to identify reactive and reverse reactive systems. From this result, we are able to divide state space into regions that characterize the reactivity of $D[F(x)]$, and hence the range of possible transient behavior. See Example 3.17 and Figure 3.4a.

Example 3.17. Let's continue our calculations from Example 3.4. Recall that we are working with the Lotka-Voltera system given by:

$$\frac{dX}{dt} = F(x,y) = \begin{pmatrix} f(x,y) \\ g(x,y) \end{pmatrix} = \begin{pmatrix} 0.09x\left(1 - \dfrac{x-y}{3}\right) \\ 0.18y\left(1 - \dfrac{y-2x}{6}\right) \end{pmatrix}$$

We had found that the Jacobian of this vector field at an arbitrary point (x, y) is given by:

$$D[F(x,y)] = \begin{pmatrix} 0.09 - 0.06x - 0.03y & -0.03x \\ -0.06y & 0.18 - 0.06x - 0.06y \end{pmatrix} \tag{3.14}$$

Figure 3.2 gave a visualization of the asymptotic stability classification regions of this system that were generated by applying the trace-determinant criteria to the Jacobian matrix (Equation 3.14). Now we are interested in characterizing state space based on the range of possible transient behavior. That is, we want to use the Hermitian part of the Jacobian to determine which regions of state space correspond to reactive, non reactive, reverse reactive, or reverse non-reactive linearizations. To do this, we must first calculate the Hermitian part of the Jacobian as well as its trace and determinant.

The Hermitian part of the Jacobian is given by:

$$\begin{aligned} H(D[F(x,y)]) &= \tfrac{1}{2}\left(D[F] + D[F]^T\right) \\ &= \begin{pmatrix} 0.09 - 0.06x - 0.03y & \frac{1}{2}\left(-0.03x - 0.06y\right) \\ \frac{1}{2}\left(-0.03x - 0.06y\right) & 0.18 - 0.06x - 0.06y \end{pmatrix} \end{aligned}$$

The trace and determinant of the Hermitian part are give by:

$$\begin{aligned} \operatorname{tr}(H(D[F(x,y)])) &= (0.09 - 0.06x - 0.03y) + (0.18 - 0.06x - 0.06y) \\ &= 0.27 - 0.12x - 0.09y \\ \det(H(D[F(x,y)])) &= (0.09 - 0.06x - 0.03y)(0.18 - 0.06x - 0.06y) - \left(\tfrac{1}{2}\left(-0.03x - 0.06y\right)\right)^2 \\ &= 0.0036(4.5 - 4.5x + 1.x^2 - 3.y + 1.xy + 0.5y^2) \end{aligned}$$

We can now apply Lemma 3.16 to determine in what regions of state space the instantaneous linear approximation is reactive or reverse reactive. For illustration, let's consider the set of inequalities (2) for the non-reactive condition.

Suppose that the instantaneous linearization at the point (x, y) satisfies the following inequalities:

$$\begin{aligned} \det(H(D[F(x,y)])) &= 0.0036(4.5 - 4.5x + 1.x^2 - 3.y + 1.xy + 0.5y^2) > 0 \\ \operatorname{tr}(H(D[F(x,y)])) &= 0.27 - 0.12x - 0.09y < 0 \end{aligned}$$

Then, at the point (x, y) the Hermitian part of the Jacobian has two negative eigenvalues. This means that the instantaneous linear approximation about (x, y) is non-reactive and reverse reactive (see the white region in Figure 3.4a).

This process can be carried out for the other two regions given by inequalities (1) and

(3) in Lemma 3.16. In Figure 3.4a, systems that are both reactive and reverse reactive are shown in blue while systems that are reactive but reverse non-reactive are shown in red.

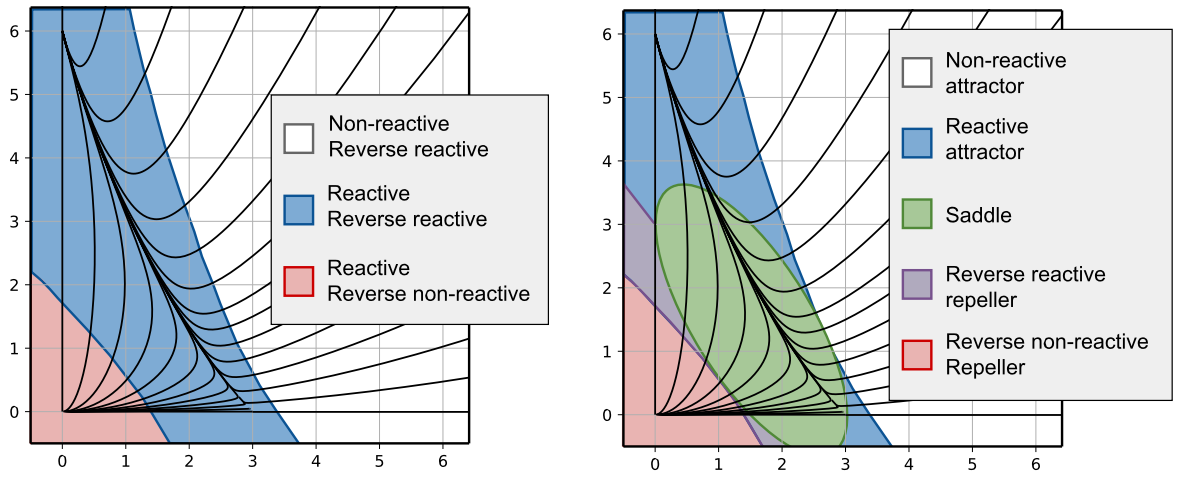

Figure 3.6: Both figures show the phase portrait for the system given in Example 3.17. (a) The figure shows state space broken into regions that describe the extremes of transient behavior. (b) We can combine the stability classification regions from Figure 3.2 with the regions in the figure on the left. The result is shown in the figure on the right. Of particular interest is the white region in which linearizations show non-reactive attraction.

Via the process outlined in Example 3.17, we obtain a region-by-region characterization of the possible transient behavior exhibited by the instantaneous linear approximations to $\frac{dX}{dt} = F(X)$ at points in state space. This is what we wanted when we first defined reactivity! We can now cross-reference the asymptotic behavior of a linearization with the possible transient behavior to gain a more accurate view of the behavior a system may contribute to the variational equation.

As we go about this process of cross-referencing asymptotic with transient behavior, it is important to keep in mind that our primary concern is whether the transient behavior can differ from the asymptotic behavior. Corollary 3.19 will state that repelling systems are, by default, reactive, just as attracting systems are, by default, reverse reactive. For this reason, we are concerned about the relationship between attracting systems and reactivity and the relationship between repelling systems and reverse reactivity.

With this in mind, in Figure 3.4b, the relevant reactivity characterizations regions are superimposed on the asymptotic classification regions. In particular we can see the white region in which instantaneous linearizations of the underlying flow are both attracting and non-reactive and the blue region in which these linearizations are attracting but reactive. Based on our previous concerns about Conjecture 3.5, the ability to distinguish between linearizations that may have transient repelling behavior and those that most certainly don't is significant. In the next section we will prove that if an equilibrium trajectory is contained entirely within this non-reactive attracting region, then the flow-kick equilibrium is itself attracting.

3.5 Analytic Characterization Results

In this section, we find analytic criteria under which Conjecture 3.5 is true. Before we present these results, it is helpful to outline when our characterization of a system's transient behavior inherently implies a particular asymptotic classification or vice versa. For example, if a system is non-reactive, then the radial velocity of all solutions at all moments in time is bounded above by zero. This precludes any repelling behavior whatsoever; the only asymptotic behavior any solution could possibly display is attraction. This statement and similar statements about the relationship between reactivity classifications and asymptotic classifications are given in Lemma 3.18 and Corollary 3.19.

Lemma 3.18. *Consider an autonomous, linear system* $\frac{dX}{dt} = AX$.

1. *If A is non-reactive, then the equilibrium attracts solutions monotonically by the norm, and the system is attracting.*
2. *If A is not reverse reactive, then the equilibrium repels solutions monotonically by the norm, and the system is repelling.*

Proof. We will present a proof for the first claim. The second claim follows similarly.

Suppose that A is non-reactive. Consider a solution $X(t)$ to $\frac{dX}{dt} = AX$ with initial value $X_0 \neq 0$. Note that because the system is linear, $X^*(t) = 0$ is an equilibrium solution and by

uniqueness $X(t)$ is non-zero for all $t \in \mathbb{R}$. Then for each $s \in \mathbb{R}$, we can write

$$X(s) = ||X(s)||\hat{X}_s \qquad \text{where} \qquad \hat{X}_s = \frac{X(s)}{||X(s)||}$$

Recall from the proof of Theorem 3.11 that in a linear setting, we can write:

$$\frac{d||X||}{dt} = \frac{1}{||X||} X^T H(A) X$$

The above equation shows that the rate of change of the norm inherits linearity from the differential equation. In particular, if we let $\hat{X}_s(t)$ represent the solution of the system through $\hat{X}_s(0) = \hat{X}_s$, this means that for any $s \in \mathbb{R}$ we can write:

$$\frac{d||X||}{dt}\Big|_{t=s} = ||X(s)|| \cdot \frac{d||\hat{X}_s(t)||}{dt}\Big|_{t=0}$$

Now we can use the fact that the system is non-reactive:

$$\begin{aligned}
\frac{d||X(t)||}{dt}\Big|_{t=s} &= ||X(s)|| \cdot \frac{d||\hat{X}_s(t)||}{dt}\Big|_{t=0} \\
&\leq ||X(s)|| \cdot \max_{||X_0||=1} \left\{ \frac{d||X||}{dt}\Big|_{t=0} \right\} \\
&= ||X(s)|| \cdot \rho(A) < 0
\end{aligned}$$

Since the above inequality is true for all $s \in \mathbb{R}$ and for any non-zero choice of the initial condition X_0, all solutions to the system always move toward the origin. This means that the origin is attracting every solution monotonically by the norm and is thus an attracting equilibrium of the system.

Note that this proof is equivalent to proving that the Euclidean norm $||\cdot||$ is a Lyapunov function [5]. □

Corollary 3.19. *Consider an autonomous, linear system* $\frac{dX}{dt} = AX$.

If the system is repelling, then it is reactive.

If the system is attracting, then it is reverse reactive.

Proof. By the contrapositive of Lemma 3.18, any system that is not attracting is reactive. Thus if a system is repelling, it will also be reactive.

Similarly, any system that is not repelling is reverse reactive. Thus if a system is attracting, it will also be reverse reactive. □

Corollary 3.19 formalizes our intuition that reactivity and reverse reactivity are, for our purposes, inconsequential in repelling and attracting systems respectively. Lemma 3.18 formalizes our intuition that non-reactive systems are those for which we can expect not only asymptotic, but also transient, attracting behavior. This result and the corresponding result for reverse non-reactive systems is important for identifying regions in which Conjecture 3.5 holds. Before we prove that Conjecture 3.5 holds under these additional criteria, we will prove a similar claim generalized to non-autonomous linear systems.

Theorem 3.20. *Consider a non-autonomous linear differential equation*

$$\frac{dX}{dt} = A(t)X \tag{3.15}$$

If, for all $\alpha \in [0, \tau]$, the autonomous linear differential equation given by

$$\frac{dX}{dt} = A(\alpha)X \tag{3.16}$$

is non-reactive, then the time-τ map ϕ_τ of the non-autonomous system 3.15 has an attracting equilibrium at the origin.

Proof. We will begin by showing that every solution to Equation 3.15 is a strictly decreasing function by the norm.

For each $\alpha \in [0, \tau]$, consider the system as given in Equation 3.16. Let $Y_\alpha(t)$ be the solution to Equation 3.16 with initial condition $Y_\alpha(0)$. Since $A(\alpha)$ is non-reactive, Lemma 3.18 tells us that for all initial conditions $Y_\alpha(0)$ and for all $t \in \mathbb{R}$,

$$\frac{d||Y_\alpha(t)||}{dt} < 0$$

Consider again the non-autonomous system given in Equation 3.15. Let $X(t)$ be the solution to Equation 3.15 with initial condition X_0. For each $\alpha \in [0, \tau]$, let $Y_\alpha(t)$ be the solution to Equation 3.16 as before, but now with initial condition $Y_\alpha(0) = X(\alpha)$.

$$\begin{aligned}
\frac{d||X(t)||}{dt}\Big|_{t=s} &= \frac{d}{dt}\left[\sqrt{X(t)^T X(t)}\right]\Big|_{t=s} \\
&= \frac{1}{2}\frac{X(s)^T \frac{dX}{dt}\Big|_{t=s} + \left(\frac{dX}{dt}\right)\Big|_{t=s}^{T} X(s)}{\sqrt{X(s)^T X(s)}} \\
&= \frac{1}{2}\frac{X(s)^T A(s) X(s) + X(s)^T A(s)^T X(s)}{\sqrt{X(s)^T X(s)}} \\
&= \frac{1}{2}\frac{Y_s(0)^T A(s) Y_s(0) + Y_s(0)^T A(s)^T Y_s(0)}{\sqrt{Y_s(0)^T Y_s(0)}} \\
&= \frac{d}{dt}\left[\sqrt{Y_s(t)^T Y_s(t)}\right]_{t=0} \\
&= \frac{d||Y_s(t)||}{dt}\Big|_{t=0}
\end{aligned}$$

Thus

$$\frac{d||Y_s||}{dt}\Big|_{t=0} < 0 \;\; \forall\, s \in [0,\tau] \quad \Longrightarrow \quad \frac{d||X(t)||}{dt} < 0 \;\; \forall\, t \in [0,\tau]$$

and $X(t)$ is a strictly decreasing function by the norm on the interval $[0,\tau]$.

Consider the time-τ map ϕ_τ of the non-autonomous system 3.15. Since $||X(t)||$ is a decreasing function for any initial condition X_0, we have in particular that $||\phi_\tau(X_0)|| < ||X_0||$. Thus one iteration of the time-τ map brings any point in state space closer to the origin.

Consider the orbit $\{\phi_\tau^n(X_0)\}$ generated by iterating the time-τ map on any seed $X_0 \in \mathbb{R}^2$. Since the norm of the points in this orbit is monotonically decreasing and bounded below by zero, we can say that:

$$\lim_{n\to\infty} ||\phi_\tau^n(X_0)|| = \widetilde{x}$$

Similarly since $\{\phi_\tau^n(X_0)\}$ is bounded, we can, by the Bolzano-Wierstrass Theorem, find a subsequence $\{\phi_\tau^m(X_0)\}_{m\in M}$ that converges to some point $\widetilde{X}$. Since $||\phi_\tau^n(X_0)|| \to \widetilde{x}$, we also know that $||\phi_\tau^m(X_0)||_{m\in M} \to \widetilde{x}$. Thus, by the continuity of the norm, $||\widetilde{X}|| = \widetilde{x}$.

Now consider applying the time-τ map to every point in the subsequence to get a new subsequence $\{\phi_\tau^{m+1}(X_0)\}_{m\in M}$. By continuity of the time-*tau* map, we know that this new subsequence must converge to $\phi_\tau(\widetilde{X})$.

Suppose for the purpose of contradiction that $\widetilde{x} \neq 0$. Then $\widetilde{X} \neq 0$ so $||\phi_\tau(\widetilde{X})|| < ||\widetilde{X}|| = \widetilde{x}$, but $||\phi_\tau^{m+1}(X_0)||_{m\in M} \to \widetilde{x}$. This is a contradiction. Therefore $\widetilde{x} = 0$ for all seeds $X_0 \in \mathbb{R}^2$.

Thus, we have that the orbit of the time-τ map for any seed X_0 is attracted to the origin, and the origin is an attracting equilibrium of the time-τ map. □

Corollary 3.21. *Consider the flow-kick system generated by F with flow time τ and flow-kick equilibrium X^*. If, for all $\alpha \in [0, \tau]$, the instantaneous linear approximation about $\phi(\alpha, X^*)$ is non-reactive, then X^* is an attracting flow-kick equilibrium.*

Proof. Consider the variational equation generated by the vector field F about the equilibrium trajectory $\phi(t, X^*)$. Suppose that the instantaneous linear approximations about each point on the equilibrium trajectory is non-reactive. Then we can apply Theorem 3.20 to say that system generated by the variational time-τ map U_τ has an attracting equilibrium at the origin.

Recall that the variational time-τ map is the linearization of the flow-kick map. This means that the orbits generated by the time-τ map linearly approximated the evolution of perturbations from the flow-kick equilibrium X^* as the system undergoes many iterations of the flow-kick map. Since the variational origin is attracting, every solution to the flow-kick system with an initial condition sufficiently close to X^* is attracted to it. Thus we classify X^* as an attracting flow-kick equilibrium. □

Theorem 3.20 and Corollary 3.21 confirm that the cumulative dynamics that arise by piecing together non-reactive systems instantaneously in time is attraction. In particular Corollary 3.21 shows that, under the extra assumption that the equilibrium trajectory is entirely contained within the *non-reactive* attracting region, the first claim of Conjecture 3.5 holds. In Theorem 3.22 and Corollary 3.23 we state the corresponding results for reverse non-reactive systems.

Theorem 3.22. *Consider a non-autonomous linear differential equation as in Equation 3.15. If, for all $\alpha \in [0, \tau]$, the autonomous linear differential equation given by Equation 3.16 is reverse non-reactive, then the time-τ map ϕ_τ of the non-autonomous system 3.15 has a repelling equilibrium at the origin.*

Corollary 3.23. *Consider the flow-kick system generated by F with flow time τ and flow-kick equilibrium X^*. If, for all $\alpha \in [0, \tau]$, the instantaneous linear approximation about $\phi(\alpha, X^*)$ is reverse non-reactive, then X^* is a repelling flow-kick equilibrium.*

The proof of Theorem 3.22 follows similarly to the proof of Theorem 3.20, just as the proof of Corollary 3.23 follows similarly to that of Corollary 3.21.

With the results from this section, we have seen that the reactivity and reverse reactivity of the instantaneous linearizations along a trajectory of $\frac{dX}{dt} = F(X)$ indicate what kind of transient behavior may be contributed to the variational equation along that trajectory. We have also identified two regions of state space in which we can be confident that the transient behavior cannot differ from the asymptotic classification. Within each of those regions, we have proved Conjecture 3.5, showing that characterizing the behavior of the instantaneous linear approximations along the equilibrium trajectory of a flow-kick system *can* tell us about the cumulative dynamical behavior of the variational equation along that trajectory. We have also identified regions of state space where the transient behavior may differ from the asymptotic classification, and in which Conjecture 3.5 remains open. In the next chapter we will continue to explore how to characterize the transient radial motion of linear systems so as to further identify criteria under which reactive or reverse reactive behavior may be instantaneously contributed to the dynamics of a non-autonomous linear system.

Chapter 4

A Radial and Tangential Velocity Approach to Classification

4.1 Introduction

In our exploration of Conjecture 3.5 so far, we have described what we will refer to in this chapter as the *eigenvalue approach* to analyzing the variational equation along a flow-kick equilibrium trajectory. This is the process of finding the eigenvalues of each instantaneous linear approximation along the equilibrium trajectory and using the classification of each approximation to deduce the classification of the variational time-τ map. As we were developing this view of the variational equation, we realized that the eigenvalue approach is incomplete because of the asymptotic nature of eigenvalue analysis and the transient role that each approximation plays in the cumulative dynamics of the variational equation. To address that issue, we introduced the concept of reactivity and reverse reactivity which describe the extremes of the *transient* behavior exhibited by a linear system.

In this chapter, we will develop a *radial and tangential velocity approach* to understanding the transient behavior that each instantaneous linear approximation along the equilibrium trajectory may potentially contribute to the variational equation. It has surprising and insightful connections to the method of calculating the reactivity presented in Theorem 3.11, and will lead us, in the next chapter, to further our exploration of the reactive attracting region of equilibrium space where Conjecture 3.5 remains open.

The radial velocity approach captures the idea that what we are really trying to determine while analyzing the variational equation is whether trajectories get closer to the variational origin or further away from the variational origin. Note that "closer to" and "further away from" are statements intrinsically about radial distance. As we analyze the variational equation we want to know: is the radial displacement positive or negative? Is the cumulative effect of the radial velocity across these approximations positive or negative?

An immediate benefit of this approach is that we can view the radial contribution of the *transient* behavior of solutions. In the eigenvalue approach, we tried to "factor out" the radial behavior of solutions by looking at the eigenvalues. Though the eigenvalues do characterize asymptotic radial movement, they only characterize the transient radial movement for the eigensolutions. Even the reactivity and reverse reactivity only characterize the possible extremes of transient radial movement. When we take the radial velocity approach, we are going directly to the source of radial movement and trying to determine the overall time-τ radial displacement. Instead of asking what eigenvalues say about the asymptotic radial movement of each approximation or even the extremes of the transient radial movement, the radial velocity approach examines the full array of possibilities for transient radial movement at each approximation.

4.2 Calculating the Radial and Tangential Components of Velocity

Given a two-dimensional autonomous linear system $\frac{dX}{dt} = AX$, there are multiple ways to compute the radial and tangential components of the velocity. One approach is to think geometrically about how the velocity vector AX can be decomposed into perpendicular components in the radial direction and in the tangential direction as in Figure **??**. The corresponding calculation is to take the dot product of AX with a unit vector in the radial direction and a unit vector in the tangential direction to find the projection of the velocity onto these vectors.

The second approach to finding the radial and tangential velocity is to think in terms of polar coordinates. Recall that in polar coordinates we write $X = (x, y) = (r\cos\theta, r\sin\theta)$. The radial velocity is the rate of change, $\frac{dr}{dt}$, of the radius r. The tangential velocity is

related to the angular velocity $\frac{d\theta}{dt}$; the difference is that the tangential velocity is measured in terms of distance in state space, whereas the angular velocity is measured in terms of angular distance. We can convert between these two velocities easily: for a point with radius r, the tangential velocity is equal to r times the angular velocity (calculated using radians).

To compute the the radial and tangential velocity now we will use the latter approach.

Lemma 4.1. *Given a two-dimensional autonomous linear system $\frac{dX}{dt} = AX$, the radial component of the velocity is given by:*

$$\frac{dr}{dt} = \frac{r}{2}\left((a+d) + (a-d)\cos 2\theta + (b+c)\sin 2\theta\right)$$

and the tangential component of the velocity is given by:

$$r\frac{d\theta}{dt} = \frac{r}{2}\left((c-b) + (d-a)\sin 2\theta + (b+c)\cos 2\theta\right)$$

Proof. Writing the system with X in Cartesian coordinates, we have:

$$\frac{dX}{dt} = \begin{pmatrix} \frac{dx}{dt} \\ \frac{dy}{dt} \end{pmatrix} = \begin{pmatrix} a & b \\ c & d \end{pmatrix} \begin{pmatrix} x \\ y \end{pmatrix}$$

With X in polar coordinates this is:

$$\begin{pmatrix} \frac{d}{dt}\left[r\cos\theta\right] \\ \frac{d}{dt}\left[r\sin\theta\right] \end{pmatrix} = \begin{pmatrix} a & b \\ c & d \end{pmatrix} \begin{pmatrix} r\cos\theta \\ r\sin\theta \end{pmatrix} = \begin{pmatrix} ar\cos\theta + br\sin\theta \\ cr\cos\theta + dr\sin\theta \end{pmatrix}$$

Differentiating the left hand side, yields a system of linear equations for $\frac{dr}{dt}$ and $\frac{d\theta}{dt}$:

$$\begin{aligned} & \frac{d}{dt}\left[r\cos\theta\right] = ar\cos\theta + br\sin\theta \\ \implies \quad & \frac{dr}{dt}\cos\theta - r\sin\theta\frac{d\theta}{dt} = ar\cos\theta + br\sin\theta, \qquad \text{and} \end{aligned}$$

$$\begin{aligned} & \frac{d}{dt}\left[r\sin\theta\right] = cr\cos\theta + dr\sin\theta \\ \implies \quad & \frac{dr}{dt}\sin\theta + r\cos\theta\frac{d\theta}{dt} = cr\cos\theta + dr\sin\theta \end{aligned}$$

Solving this system for $\frac{dr}{dt}$ and $\frac{d\theta}{dt}$, we have:

$$\begin{aligned} \frac{dr}{dt} &= \frac{r}{2}\left((a+d) + (a-d)\cos 2\theta + (b+c)\sin 2\theta\right) \\ \frac{d\theta}{dt} &= \frac{1}{2}\left((c-b) + (d-a)\sin 2\theta + (b+c)\cos 2\theta\right) \end{aligned}$$

and the lemma follows since the tangential velocity is given by $r\frac{d\theta}{dt}$. □

Notice that $\frac{d\theta}{dt}$ is independent of the radius and thus the tangential velocity depends on the radius only for a scaling factor. Similarly, the radial velocity, $\frac{dr}{dt}$, depends on the radius only for a scaling factor. This is a consequence of the linearity of the system. As such, we can characterize the radial and tangential transient movement of all solutions while restricting attention to the unit circle.

Definition 4.2. *Given a two-dimensional autonomous linear system $\frac{dX}{dt} = AX$, we let $\mathcal{R} : \mathbb{R} \to \mathbb{R}$ denote the radial component of the velocity on the unit circle, given by:*

$$\mathcal{R}(\theta) = \frac{dr}{dt}\Big|_{r=1} = \frac{1}{2}\left((a+d) + (a-d)\cos 2\theta + (b+c)\sin 2\theta\right)$$

and we let $\mathcal{T} : \mathbb{R} \to \mathbb{R}$ denote the tangential component of the velocity on the unit circle given by:

$$\mathcal{T}(\theta) = r\frac{d\theta}{dt}\Big|_{r=1} = \frac{1}{2}\left((c-b) + (d-a)\sin 2\theta + (b+c)\cos 2\theta\right)$$

Now that we have equations for the radial and tangential components of the velocity, we can use graphical and algebraic manipulation to observe certain properties about them. We will start by underlining some of the intrinsic properties of $\mathcal{R}$ and $\mathcal{T}$ we can draw from their algebraic form.

First we notice that both the radial and tangential components have a vertical shift which is independent of the position on the unit circle: $\mathcal{R}$ is shifted up by $\frac{1}{2}(a+d)$ and $\mathcal{T}$ is shifted up by $\frac{1}{2}(c-b)$. We will consider these vertical shifts to be the *baseline radial movement* in the case of $\mathcal{R}$ and the *baseline rotation* in the case of $\mathcal{T}$.

Next we describe, in Theorems 4.3 and 4.4, the tight relationship between $\mathcal{R}(\theta)$ and $\mathcal{T}(\theta)$.

Theorem 4.3. *For a two-dimensional autonomous linear system $\frac{dX}{dt} = AX$, if the matrix $A = \left(\begin{smallmatrix} a & b \\ c & d \end{smallmatrix}\right)$ has $a \neq d$ or $b \neq -c$, then the radial and tangential components of the velocity on the unit circle have the following properties:*

(i) $\mathcal{R}(\theta)$ and $\mathcal{T}(\theta)$ are both sinusoidal functions with period π.

(ii) The oscillations of $\mathcal{R}(\theta)$ and $\mathcal{T}(\theta)$ have the same amplitude.

(iii) The oscillations of $\mathcal{T}(\theta)$ are related to the oscillations of $\mathcal{R}(\theta)$ by a phase shift of $\frac{\pi}{4}$.

Proof. To prove property (i), notice that the modulation of both the radial and tangential velocity along the unit circle is dependent on two trigonometric functions. In both cases, the trigonometric functions have matching periods of π. This means that the sum of the trigonometric functions will also be periodic with period π. Thus, $\mathcal{R}$ and $\mathcal{T}$ are sinusoidal functions with period π. This is not unexpected since we know that the linearity of the underlying system creates symmetry across the origin. Finally, we note that the hypotheses on the coefficients of A ensure that $\mathcal{R}$ and $\mathcal{T}$ are not constant functions.

To prove properties (ii) and (iii), we must first notice the similarities between the coefficients in $\mathcal{R}$ and $\mathcal{T}$. The sine coefficient of $\mathcal{T}$ is equal to the negative of the cosine coefficient of $\mathcal{R}$, while the cosine coefficient of $\mathcal{T}$ is equal to the sine coefficient of $\mathcal{T}$. This observation is highlighted in the equations below:

$$\mathcal{R}(\theta) = \frac{1}{2}(a+d) + \frac{1}{2}\Big((a-d) \cos 2\theta + (b+c) \sin 2\theta \Big)$$
$$\mathcal{T}(\theta) = \frac{1}{2}(c-b) + \frac{1}{2}\Big(-(a-d) \sin 2\theta + (b+c) \cos 2\theta \Big)$$

Recall that sine and cosine are equivalent up to a phase shift:

$$\sin(x) = -\cos(x + \tfrac{\pi}{2}) \qquad \text{and} \qquad \cos(x) = \sin(x + \tfrac{\pi}{2})$$

Using this trigonometric identity, we can show that the modulation of $\mathcal{T}$ is, in fact, equivalent to the modulation of $\mathcal{R}$ shifted by $\frac{\pi}{4}$.

$$\sin(2\theta) = -\cos(2\theta + \tfrac{\pi}{2}) = -\cos(2(\theta + \tfrac{\pi}{4}))$$
$$\cos(2\theta) = \sin(2\theta + \tfrac{\pi}{2}) = \sin(2(\theta + \tfrac{\pi}{4}))$$

and thus

$$\mathcal{R}(\theta) = \frac{1}{2}(a+d) + \frac{1}{2}\big((a-d)\cos 2\theta \qquad + (b+c)\sin 2\theta\big)$$
$$\mathcal{T}(\theta) = \frac{1}{2}(c-b) + \frac{1}{2}\big((a-d)\cos(2(\theta+\tfrac{\pi}{4})) + (b+c)\sin(2(\theta+\tfrac{\pi}{4}))\big)$$

Properties (ii) and (iii) follow directly from these equations. □

Summarizing: in the case when either $a \neq d$ or $b \neq -c$, $\mathcal{R}$ and $\mathcal{T}$ both take the form of sinusoidal functions of period π, with the same amplitude, but translated vertically by

different amounts. They are related to each other by a phase shift of $\frac{\pi}{4}$, so that each reaches its extremes as the other passes through its midpoint.

In Theorem 4.4 we show that in the remaining case, when $a = d = \alpha$ and $b = -c = -\beta$, the radial and tangential components of the velocity are constant for all θ. These dynamics are to be expected since matrices of the form $\left(\begin{smallmatrix} \alpha & -\beta \\ \beta & \alpha \end{smallmatrix}\right)$ are in canonical form, and yield systems that spiral around the origin with perfect rotational symmetry [5].

Theorem 4.4. *Consider a matrix A of the form $\left(\begin{smallmatrix} \alpha & -\beta \\ \beta & \alpha \end{smallmatrix}\right)$. Then the radial velocity is equal to α and tangential velocity is equal to β for all points on the unit circle.*

Proof. We will prove this claim from two perspectives.

Firstly, the result follows immediately from Definition 4.2:

$$\mathcal{R}(\theta) = \frac{1}{2}(\alpha + \alpha) + \frac{1}{2}((\alpha - \alpha)\cos 2\theta + (-\beta + \beta)\sin 2\theta) = \alpha$$
$$\mathcal{T}(\theta) = \frac{1}{2}(\beta + \beta) + \frac{1}{2}\left((\alpha - \alpha)\cos(2(\theta + \tfrac{\pi}{4})) + (-\beta + \beta)\sin(2(\theta + \tfrac{\pi}{4}))\right) = \beta$$

Secondly, from a dynamical systems perspective, we know that the general solution to linear systems of this form is given by:

$$X(t) = c_1 e^{\alpha t}\begin{pmatrix} \cos\beta t \\ -\sin\beta t \end{pmatrix} + c_2 e^{\alpha t}\begin{pmatrix} \sin\beta t \\ \cos\beta t \end{pmatrix}$$

Thus solutions spiral uniformly around the origin with angular velocity β and normalized radial velocity α. Recall from Definition 4.2 that the tangential velocity $\mathcal{T}(\theta)$ on the unit circle is equal to the angular velocity. Similarly, the normalized radial velocity is precisely the radial velocity on the unit circle. □

Corollary 4.5. *Consider a skew-symmetric matrix $A = \left(\begin{smallmatrix} 0 & -\beta \\ \beta & 0 \end{smallmatrix}\right)$. Then the radial velocity is equal to zero and the tangential velocity is equal to β for all points on the unit circle.*

In the previous section we discussed how the radial and tangential approach has the benefit of extracting transient radial behavior of the system from the rest of the dynamics. From Theorems 4.3 and 4.4 we now know that the radial and tangential approach also reveals an intriguing underlying structure relating the transient radial and tangential behavior, as illustrated in Figure 4.2. In the next section we will explore how this structure relates to the reactivity and reverse reactivity defined in Chapter 3.

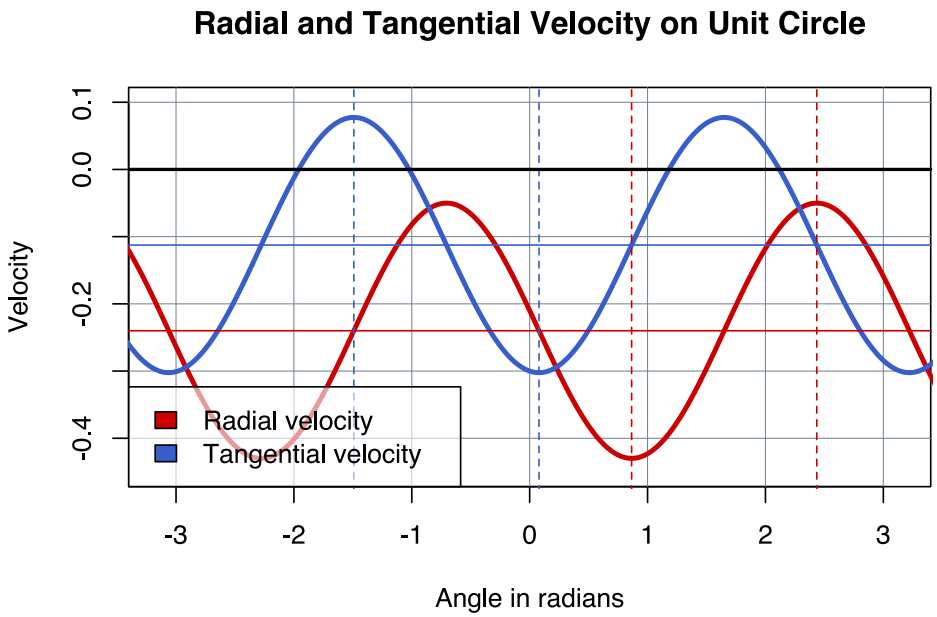

Figure 4.1: The horizontal red line shows the midpoint of the radial velocity oscillations. Similarly the horizontal blue line shows the midpoint of the tangential velocity oscillations. The vertical dashed lines show that the extremes of each oscillation occur at the same time as the midpoint of the other oscillation.

4.3 Radial Velocity and the Hermitian Matrix

Recall that reactivity is defined as the maximum radial velocity on the unit circle of a linear system $\frac{dX}{dt} = AX$. In Definition 3.7, we wrote:

$$\rho(A) = \max_{||X_0||=1} \left\{ \frac{d||X||}{dt}\Big|_{t=0} \right\}$$

Now, with our new notation, we can write:

$$\rho(A) = \max_{0 \leq \theta < \pi} \{\mathcal{R}(\theta)\}$$

Similarly, reverse reactivity is defined as the minimum radial velocity on the unit circle and can now be written:

$$\sigma(A) = \min_{0 \leq \theta < \pi} \{\mathcal{R}(\theta)\}$$

Recall from Theorems 3.11 and 3.13 that reactivity and reverse reactivity are calculated by finding the eigenvalues of the Hermitian part of the coefficient matrix A. This implies that the asymptotic characteristics of the linear system corresponding to Hermitian part of A have some relationship with the transient radial and tangential behavior of the linear system corresponding to A.

This section aims to break down that relationship so as to create an elegant framework for understanding Theorems 3.11 and 3.13 and for analytically constructing $\mathcal{R}(\theta)$ and $\mathcal{T}(\theta)$.

To begin, let's formalize the systems we are working with. Recall from Definition 3.10 that the Hermitian and antihermitian parts of A form an arithmetic decomposition of A into symmetric and skew-symmetric components:

$$A = H(A) + S(A)$$

Note that this decomposition can also be applied to the linear system corresponding to A:

$$\frac{dX}{dt} = AX = H(A)X + S(A)X \tag{4.1}$$

Thus we can think about the dynamics that arise from the linear systems corresponding to $H(A)$ and $S(A)$ as components of the dynamics arising from Equation 4.1.

$$\frac{dX}{dt} = H(A)X \tag{4.2}$$

$$\frac{dX}{dt} = S(A)X \tag{4.3}$$

In particular, Lemma 4.6 tells us that we can also think about the radial and tangential components of 4.2 and 4.3 forming a decomposition of the radial and tangential components of 4.1.

Lemma 4.6. *Let $A \in M_2(\mathbb{R})$ be a real 2×2 matrix. Let $\mathcal{R}_H$ and $\mathcal{T}_H$ represent the radial and tangential components of the Hermitian system given by Equation 4.2. Similarly let $\mathcal{R}_S$ and $\mathcal{T}_S$ represent the radial and tangential components of the skew-symmetric system by Equation 4.3. For all $\theta \in [-\pi, \pi]$,*

$$\mathcal{R}_H(\theta) + \mathcal{R}_S(\theta) = \mathcal{R}(\theta)$$
$$\mathcal{T}_H(\theta) + \mathcal{T}_S(\theta) = \mathcal{T}(\theta)$$

Proof. Let the Hermitian matrix $H(A)$ be represented by the the matrix $\left(\begin{smallmatrix} a_H & b_H \\ c_H & d_H \end{smallmatrix}\right)$ and the skew-symmetric matrix $S(A)$ be represented by the the matrix $\left(\begin{smallmatrix} a_S & b_S \\ c_S & d_S \end{smallmatrix}\right)$. Then, because $A = H(A) + S(A)$, we can write:

$$\begin{pmatrix} a & b \\ c & d \end{pmatrix} = \begin{pmatrix} a_H + a_S & b_H + b_S \\ c_H + c_S & d_H + d_S \end{pmatrix}$$

Notice that the radial velocity (as given in Definition 4.2) is linear with respect to the coefficients a, b, c, and d. Thus the sum $\mathcal{R}_H(\theta) + \mathcal{R}_S(\theta)$ can be refactored:

$$\begin{aligned} \mathcal{R}_H(\theta) + \mathcal{R}_S(\theta) &= \frac{1}{2}\left((a_H + d_H) + (a_H - d_H)\cos 2\theta + (b_H + c_H)\sin 2\theta\right) \\ &\quad + \frac{1}{2}\left((a_S + d_S) + (a_S - d_S)\cos 2\theta + (b_S + c_S)\sin 2\theta\right) \\ &= \frac{1}{2}\left((a + d) + (a - d)\cos 2\theta + (b + c)\sin 2\theta\right) = \mathcal{R}(\theta) \end{aligned}$$

The second claim follows similarly. □

Now that we know the dynamics arising from $H(A)$ and $S(A)$ sum to the dynamics of A, we want to know what kind of dynamics each component of the decomposition extracts from the dynamics of A. We already know from Theorems 3.11 and 3.13 that the eigenvalues of $H(A)$ reveal the maximum and minimum radial velocity. Let's construct some intuition about what drives this relationship by using our radial and tangential framework.

To begin, we ask the question: how do our eigenvalues and eigenvectors fit into this approach? We answer this question in the following three results.

Lemma 4.7. *Let $A \in M_2(\mathbb{R})$. Consider the autonomous linear system $\frac{dX}{dt} = AX$. If there exists $\theta_v \in [0, \pi]$ such that $\mathcal{T}(\theta_v) = 0$, then for all $r \in \mathbb{R}$, $V = \left(\begin{smallmatrix} r\cos\theta_v \\ r\sin\theta_v \end{smallmatrix}\right)$ is a real eigenvector with real eigenvalue $\mathcal{R}(\theta_v)$.*

Proof. Suppose that for some $\theta_v \in [-\pi, \pi]$, $T(\theta_v) = 0$. Let $V = \left(\begin{smallmatrix} \cos\theta_v \\ \sin\theta_v \end{smallmatrix}\right)$. Then, since there is no tangential component of the velocity, $\frac{dV}{dt} = AV$ is entirely in the radial direction. This means that the radial velocity is equal to the magnitude of the velocity at V:

$$\mathcal{R}(\theta_v) = ||AV||$$

Similarly, because the velocity is *only* radial, we can write:

$$\frac{dV}{dt} = \mathcal{R}(\theta_v)V$$

Thus V is a unit eigenvector with eigenvalue $\lambda = \mathcal{R}(\theta)$.

Because real eigenvectors lie along a line, this also means that any vectors $rV = \begin{pmatrix} r\cos\theta_v \\ r\sin\theta_v \end{pmatrix}$ are eigenvectors with the same eigenvalue $\mathcal{R}(\theta_v)$. □

Lemma 4.7 says that anytime $\mathcal{T}(\theta) = 0$, we have a real eigenvector with angle θ and real eigenvalue $\lambda = \mathcal{R}(\theta)$. In the next lemma we show that the converse is also true.

Lemma 4.8. *Consider a system $\frac{dX}{dt} = AX$ such that $A \in M_2(\mathbb{R})$ has real eigenvectors V_1, V_2 and eigenvalues $\lambda_1 \neq \lambda_2$. Let θ_1, θ_2 be the angles corresponding to the eigenvalues. Then $\mathcal{T}(\theta_1) = \mathcal{T}(\theta_2) = 0$, $\mathcal{R}(\theta_1) = \lambda_1$ and $\mathcal{R}(\theta_2) = \lambda_2$*

Proof. Consider V_1. Since eigenvectors are only unique up to scalar multiplication, we can assume, without loss of generality, that $||V_1|| = 1$. Since V_1 is an eigenvector we can write its velocity as

$$\frac{dV_1}{dt} = AV_1 = \lambda_1 V_1$$

Note that the radial direction at a point X is the vector from 0 to X. Thus, since the velocity at V_1 is in the direction of V_1, the velocity *is* the radial velocity. So we have that $\mathcal{T}(\theta_1) = 0$ and $\mathcal{R}(\theta_1) = ||\lambda_1 V_1|| = \lambda_1$.

The same argument can be applied to the second real eigenpair. □

Thus, for systems with real eigenvalues and eigenvectors, the eigenpairs can be found in our radial and tangential approach by looking for where $\mathcal{T}(\theta) = 0$. We can't necessarily "find" complex eigenvectors and eigenvalues in the same way, however our result for real eigenpairs leads directly to the result that systems with complex eigenvalues and eigenvectors can never have $\mathcal{T}(\theta) = 0$:

Corollary 4.9. *Let $A \in M_2(\mathbb{R})$. Consider its corresponding linear system $\frac{dX}{dt} = AX$. A has complex eigenvector and eigenvalues if and only if $\mathcal{T}(\theta) \neq 0$ for all $\theta \in [0, \pi]$.*

Proof. The forward direction is the contrapositive of Lemma 4.7: if A doesn't have real eigenvectors and eigenvalues, then $\mathcal{T}(\theta)$ cannot have zeros.

The backward implication is the contrapositive of Lemma 4.8: if $\mathcal{T}(\theta)$ has no zeros, then A cannot have real eigenvalues and eigenvectors. □

Corollary 4.9 is consistent with our observation of complex systems in canonical form from Theorem 4.4. Since the tangential velocity can never equal zero, it can never switch sign. Solutions spiral entirely clockwise or entirely counter clockwise in the phase plane.

Now that we have an understanding of how the eigenvalues and eigenvectors of a system appear in the radial and tangential approach, we want to uncover the role that the eigenvalues of the Hermitian play. Let's start by considering what properties the Hermitian/antihermitian decomposition posses in particular. Recall that the Hermitian part $H(A)$ is a symmetric matrix and the antihermitian part $S(A)$ is a skew-symmetric matrix.

Corollary 4.5 characterizes the radial and tangential velocities of a system whose coefficient matrix is skew-symmetric like $S(A)$. By this corollary, we know that the system corresponding to $S(A)$ (given in Equation 4.3) has zero radial velocity and constant tangential velocity. This is seen for the matrix $A = \left(\begin{smallmatrix} -0.21 & -0.075 \\ -0.3 & -0.27 \end{smallmatrix}\right)$ in Figure 4.3

Now let's use our radial and tangential framework to characterize some special properties of symmetric matrices.

Lemma 4.10. *If $A \in M_2(\mathbb{R})$ is a symmetric matrix, then*

(i) A has real and orthogonal eigenvectors,

(ii) and A has real eigenvalues $\rho = \max\{\mathcal{R}(\theta)\}$ and $\sigma = \min\{\mathcal{R}(\theta)\}$.

Proof. Suppose that A is symmetric. Then we can write $A = \left(\begin{smallmatrix} a & b \\ b & d \end{smallmatrix}\right)$.

So $\mathcal{T}(\theta)$ becomes:

$$\begin{aligned} \mathcal{T}(\theta) &= \tfrac{1}{2}\left((b-b) + (a-d)\cos 2\theta + (b+b)\sin 2\theta\right) \\ &= \tfrac{1}{2}\left(a-d\right)\cos 2\theta + b\sin 2\theta \end{aligned}$$

We observe that $\mathcal{T}$ is sinusoidal with period π and has no vertical shift. In other words, $\mathcal{T}$ crosses the θ axis every $\frac{\pi}{2}$ radians. Let θ_1 and $\theta_2 = \theta_1 + \frac{\pi}{2}$ represent the angles in $[0, \pi]$ for which $\mathcal{T}(\theta) = 0$.

By Lemma 4.7, A has real eigenvectors V_1 and V_2 corresponding to θ_1 and θ_2 with real eigenvalues $\mathcal{R}(\theta_1)$ and $\mathcal{R}(\theta_2)$. Because $\theta_2 = \theta_1 + \frac{\pi}{2}$, the eigenvectors V_1 and V_2 are orthogonal. This proves statement (i).

To prove statement (ii), note again that θ_1 and θ_2 are where $\mathcal{T}$ passes the middle of its oscillation. Since, by Theorem 4.3, $\mathcal{T}(\theta)$ and $\mathcal{R}(\theta)$ are related by a phase shift of $\frac{\pi}{4}$, we know that θ_1 and θ_2 correspond to the extremes of the radial velocity $\mathcal{R}$. Thus the real eigenvalues of A are the extremes of the radial velocity: $\rho = \max\{\mathcal{R}(\theta)\}$ and $\sigma = \min\{\mathcal{R}(\theta)\}$. □

We now have a way of characterizing both the Hermitian part $H(A)$ and the antihermitian part $S(A)$ within our radial and tangential approach (see Figure 4.3). With these characterizations, we are now able to give an alternative proof of Theorems 3.11 and 3.13 using our new framework.

Theorem 4.11. *Let $A \in M_2(\mathbb{R})$. Consider the associated autonomous linear differential equation $\frac{dX}{dt} = AX$. The maximum and minimum radial velocity on the unit circle are given by the eigenvalues of the Hermitian part $H(A)$.*

Proof. Consider the decomposition of A into the Hermitian (symmetric) and antihermitian (skew-symmetric) parts: $A = S(A) + H(A)$. As in Lemma 4.6 let $\mathcal{R}_H$, $\mathcal{R}_S$, $\mathcal{T}_H$ and $\mathcal{T}_S$ be the radial and tangential components of $H(A)$ and $S(A)$ respectively.

By Lemma 4.6, we have that $\mathcal{R}_H(\theta) + \mathcal{R}_S(\theta) = \mathcal{R}(\theta)$. But, by Corollary 4.5, $\mathcal{R}_S(\theta) = 0$. Thus $\mathcal{R}_H(\theta) = \mathcal{R}(\theta)$.

Since $H(A)$ is symmetric, we know by Lemma 4.10 that its eigenvalues are the extremes of $\mathcal{R}_H(\theta)$. Since $\mathcal{R}_H = \mathcal{R}$, this means that the eigenvalues of $H(A)$ give the extremes of the radial velocity on the unit circle according to the dynamics of A. □

Though Theorem 4.11 does not present new results, it does highlight the elegance of the Hermitian/antihermitian decomposition when viewed in the radial and tangential framework.

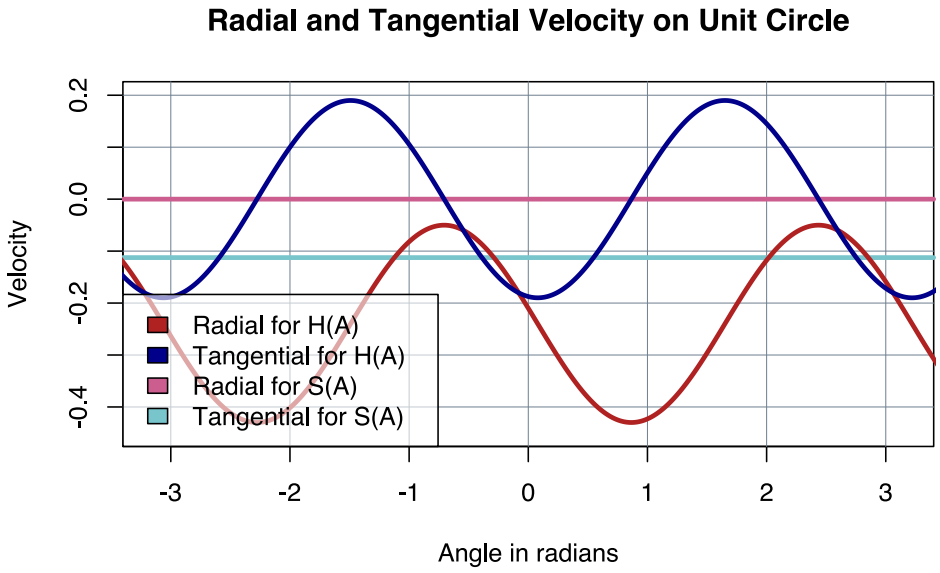

Figure 4.2: The radial velocity of $S(A)$ (shown in pink) is zero and the tangential velocity of $S(A)$ (shown in light blue) is constant. The tangential velocity of $H(A)$ (shown in dark blue) is centered around the origin. The radial velocity of $H(A)$ (shown in dark red) is the same as the radial velocity of A (see Figure 4.2).

4.4 Applying the Radial Velocity Approach

We developed this radial and tangential velocity approach to better understand the transient behavior of any given autonomous linear system $\frac{dX}{dt} = AX$. We saw through Sections 4.2 and 4.3 that the transient behavior of a linear system decomposed into its radial and tangential components has incredible structure with deep connections to the Hermitian/antihermitian decomposition of the coefficient matrix A. In the following theorem we will apply all of this structure to re-write the radial and tangential velocities in terms of the eigenvalues and eigenvectors of the Hermitian part $H(A)$ and antihermitian part $S(A)$ of the coefficient matrix A.

Theorem 4.12. *Given an autonomous linear system $\frac{dX}{dt} = AX$, consider the radial and tangential components, $\mathcal{R}(\theta)$ and $\mathcal{T}(\theta)$, of the velocity on the unit circle parameterized by*

the angle θ. We can write

$$\mathcal{R}(\theta) = \tfrac{1}{2}(\rho+\sigma) + \tfrac{1}{2}(\rho-\sigma)\cos(2(\theta-\theta_\rho)) \tag{4.4}$$

$$\mathcal{T}(\theta) = \quad \omega \quad - \tfrac{1}{2}(\rho-\sigma)\sin(2(\theta-\theta_\rho)) \tag{4.5}$$

where $\rho = \max\{\Lambda(H(A))\}$ is the reactivity, $\sigma = \min\{\Lambda(H(A))\}$ is the reverse reactivity, θ_ρ is the angle corresponding to the eigenvector of $H(A)$ with eigenvalue ρ, and ω is the constant rotation arising from $\frac{dX}{dt} = S(A)X$.

Proof. First, recall from Theorem 4.3 that $\mathcal{R}(\theta)$ and $\mathcal{T}(\theta)$ are sinusoidal with period π. Thus we can write them in the form:

$$M + A\sin(2(\theta-\theta_0)) \qquad \text{or} \qquad M + A\cos(2(\theta-\theta_{\max}))$$

where M is the midpoint or vertical shift of the oscillation, A is the amplitude of the oscillation, θ_0 is the angle for which the oscillation increases through the midpoint, and $\theta_{\max}$ is the angle for which the oscillation passes through the maximum.

From Theorem 4.3 we also know that $\mathcal{R}(\theta)$ and $\mathcal{T}(\theta)$ have the same amplitude and that $\mathcal{T}(\theta)$ is related to $\mathcal{R}(\theta)$ by a phase shift of $\frac{\pi}{4}$. Thus if we write:

$$\mathcal{R}(\theta) = M_{\mathcal{R}} + A\cos(2(\theta-\theta_{\max(\mathcal{R})}))$$

then we can also write:

$$\begin{aligned}\mathcal{T}(\theta) &= M_{\mathcal{T}} + A\cos(2((\theta+\tfrac{\pi}{4})-\theta_{\max(\mathcal{R})})) \\ &= M_{\mathcal{T}} - A\sin(2(\theta+\theta_{\max(\mathcal{R})}))\end{aligned}$$

By Theorem 4.11, the eigenvalues of $H(A)$ are the maximum and minimum values of $\mathcal{R}(\theta)$. These values are already defined as the reactivity ρ and the reverse reactivity σ. Let the angles corresponding to the eigenvectors of $H(A)$ be θ_ρ and θ_σ respectively. Note that $\theta_{\max(\mathcal{R})} = \theta_\rho$. Also note that the vertical shift of the oscillations is the average of the extremes (ie. $\frac{1}{2}(\rho+\sigma)$), and the amplitude of the oscillations is half the distance between the extremes (ie. $\frac{1}{2}(\rho-\sigma)$). Thus we can now write:

$$\begin{aligned}\mathcal{R}(\theta) &= \tfrac{1}{2}(\rho+\sigma) + \tfrac{1}{2}(\rho-\sigma)\cos(2(\theta-\theta_\rho)) \\ \mathcal{T}(\theta) &= \quad M_{\mathcal{T}} \quad - \tfrac{1}{2}(\rho-\sigma)\sin(2(\theta-\theta_\rho))\end{aligned}$$

Finally, we can find $M_{\mathcal{T}}$ in terms of the dynamics of $S(A)$ since:

1. $\mathcal{T}(\theta_\rho) = M_\mathcal{T}$ since $\mathcal{R}$ and $\mathcal{T}$ are related by a phase shift of $\frac{\pi}{4}$ (Theorem 4.3),
2. $\mathcal{T}_H(\theta_\rho) = 0$ since θ_ρ corresponds to an eigenvector of $H(A)$ (Lemma 4.8),
3. and $\mathcal{T}_H(\theta_\rho) + \mathcal{T}_S(\theta_\rho) = \mathcal{T}(\theta_\rho)$ (Lemma 4.6).

Putting these three facts together: $M_\mathcal{T} = \mathcal{T}_S(\theta_\rho)$.

We can characterize this further since $S(A)$ is a skew-symmetric matrix of the form $\left(\begin{smallmatrix} 0 & -\omega \\ \omega & 0 \end{smallmatrix}\right)$ whose corresponding dynamics have $\mathcal{T}_S(\theta) = \omega$ (by Corollary 4.5). Recall that since $S(A)$ is skew-symmetric, the corresponding system $\frac{dX}{dt} = S(A)X$ has solutions that stay at a constant radial distance from the origin but rotate with constant angular velocity ω.

With this last piece of information, we can write:

$$\begin{aligned} \mathcal{R}(\theta) &= \tfrac{1}{2}(\rho + \sigma) + \tfrac{1}{2}(\rho - \sigma)\cos(2(\theta - \theta_\rho)) \\ \mathcal{T}(\theta) &= \quad \omega \quad - \tfrac{1}{2}(\rho - \sigma)\sin(2(\theta - \theta_\rho)) \end{aligned}$$

as desired.

Note that this characterization works even in the special case where $A = \left(\begin{smallmatrix} \alpha & -\beta \\ \beta & \alpha \end{smallmatrix}\right)$, since $H(A) = \left(\begin{smallmatrix} \alpha & 0 \\ 0 & \alpha \end{smallmatrix}\right)$ has eigenvalues with algebraic multiplicity of two (ie. $\rho = \sigma = \alpha$). This means that the sinusoidal terms in the above equations would zero coefficients and we would be left with

$$\begin{aligned} \mathcal{R}(\theta) &= \rho = \sigma = \alpha \\ \mathcal{T}(\theta) &= \omega = \beta \end{aligned}$$

as desired. □

Equations 4.4 and 4.5 give a satisfying way to represent $\mathcal{R}$ and $\mathcal{T}$ in a way that explicitly relates them to the eigenvalues and eigenvectors of the Hermitian/antihermitian decomposition. This provides a way of representing $\mathcal{R}$ and $\mathcal{T}$ via a handful of symbolic calculations that is perhaps more meaningful than using the individual coefficients of the matrix A.

What does this give us? Remember that our goal is to characterize the transient behavior of autonomous linear systems so that we can understand how transient contributions piece together to create the accumulated behavior of the variational equation. In this chapter we have been thinking about the radial and tangential components of the velocity for

a single autonomous linear system. To extend this approach to how autonomous linear systems may be "strung along" non-autonomously, we can think about the time-dependent radial and tangential velocities $\mathcal{R}(\theta, t)$ and $\mathcal{T}(\theta, t)$ of a non-autonomous linear system (like the variational equation). By linearity, the time-dependent radial and tangential velocities at each time t are equivalent to the radial and tangential velocities of the corresponding instantaneous linear system. We can then write:

$$\mathcal{R}(\theta, t) = \tfrac{1}{2}(\rho(t) + \sigma(t)) + \tfrac{1}{2}(\rho(t) - \sigma(t))\cos(2(\theta - \theta_\rho(t)) \tag{4.6}$$

$$\mathcal{T}(\theta, t) = \quad \omega(t) \quad - \tfrac{1}{2}(\rho(t) - \sigma(t))\sin(2(\theta - \theta_\rho(t))) \tag{4.7}$$

Viewing the variational equation in this way gives rise to a list of natural questions about how to characterize the change in possible transient contributions over time.

1. How does $\rho(t)$ change on the interval $t \in [0, \tau]$? Is it always positive or always negative? Can we characterize $\frac{\partial \rho}{\partial t}$ or $\int_0^\tau \rho(t)dt$? Does the latter provide a bound for the overall radial repulsion on the interval $[0, \tau]$?

2. How does $\sigma(t)$ change on the interval $t \in [0, \tau]$? Is it always positive or always negative? Can we characterize $\frac{\partial \sigma}{\partial t}$ or $\int_0^\tau \sigma(t)dt$? Does the latter provide a bound for the overall radial attraction on the interval $[0, \tau]$?

3. How does $\theta_\rho(t)$ change on the interval $t \in [0, \tau]$? That is, how is the reactive direction rotating in time? Can we characterize $\frac{\partial \theta_\rho}{\partial t}$?

4. How does $\omega(t)$ change on the interval $t \in [0, \tau]$? That is, how is the average tangential velocity changing in time? Can we characterize $\frac{\partial \omega}{\partial t}$?

Addressing each of these questions would help us to understand *how* transient behavior is "strung along." Conjecture 3.5 would have that the concerted transient behavior all along the equilibrium trajectory is represented by the asymptotic classifications of each instantaneous linearization. We have proved in Theorems 3.20 and 3.22 that the accumulated asymptotic classification *does* characterize the accumulated transient behavior *if* the transient behavior is always the same as the asymptotic classification. Now we are asking: if the transient behavior can differ from the asymptotic classification, in what way does the transient behavior of the instantaneous linearizations accumulate? In particular, we want to know if it is possible for transient behavior that differs from the asymptotic behavior to

accumulate to yield an asymptotic classification of the non-autonomous system that also differs from the asymptotic behavior of all the instantaneous components. If this is possible, and we can prove the existence of a variational equation with this feature, then we will have disproved Conjecture 3.5.

In the next chapter we will use the radial and tangential velocity approach to construct an example of a non-autonomous linear differential equation that does have this property: although each instantaneous autonomous linear component of the non-autonomous system is asymptotically attracting, the non-autonomous system is not asymptotically attracting.

Chapter 5

Non-autonomous Accumulation of Asymptotic Attraction can Yield Repulsion

5.1 Introduction

In Chapter 4, we developed the radial and tangential velocity approach to better understand how to characterize the transient behavior of linear systems. In Section 4.4, we extended this approach to non-autonomous linear systems such as the variational equation. Remember that our goal in all of this is to be able to characterize the stability of any given flow-kick equilibrium. This involves being able to characterize the variational time-tau map which linearizes the flow-kick map.

This thesis works to build analytic techniques for classifying the asymptotic stability of the variational time-τ map. To work towards this goal we are now in the midst of answering the following question: does the asymptotic stability classification of each instantaneous linearization on the equilibrium trajectory imply the asymptotic stability of the variational equation? That is, can we judge the stability of a flow-kick equilibrium based purely on the eigenvalues of the instantaneous linearizations about points on its equilibrium trajectory? Conjecture 3.5 posits that the answer to both of these questions is *yes*. At the moment it is not obvious whether the conjecture is true or false. On the one hand, we have found criteria under which the conjecture does hold (Theorems 3.21 and 3.23), and we have yet to find a counterexample to disprove it. On the other hand, we also know that the instantaneous linearizations along the equilibrium trajectory contribute *transient* behavior to the variational

equation, and in some cases, such as reactive attracting systems, the transient behavior may differ from its asymptotic classification. In particular, we can conceive of a non-autonomous system composed of instantaneous reactive attracting linearizations in which the positive radial transient behavior accumulates so as to create asymptotic repulsion in the time-τ map of the non-autonomous system. In the next section we will construct an example of such a system. In Section 5.3, we will draw what conclusions we can from this constructed example and propose new research directions that will contribute to the further pursuit of our goal.

5.2 Example with positive radial velocity accumulation

In this section, we will construct an example which illustrates that the positive radial velocity of reactive systems *can* accumulate endlessly in a non-autonomous linear system leading to instability rather than attraction in the time-τ map. To begin our construction, consider the reactive attracting linear system used in Example 3.6:

$$\frac{dX}{dt} = AX = \begin{pmatrix} -1 & 10 \\ 0 & -3 \end{pmatrix} X \tag{5.1}$$

Note that A has two negative eigenvalues $\lambda_W = -1$ (the weak eigenvalue) and $\lambda_S = -3$ (the strong eigenvalue) with corresponding eigenvectors $V_W = (1, 0)$ and $V_S = (-10, 1)$.

Figure 5.2, shows the phase portrait for System (5.1). We see that most solutions start by moving roughly parallel to the strong eigenline (highlighted in purple), which takes them into the reactive region (highlighted in red). After they exit the reactive region, they approach the origin along the weak eigenline (highlighted in cyan).

Viewed algebraically: every solution can be written as the linear combination of the eigensolutions. Even though both components are decreasing (a result of two negative eigenvalues), the component corresponding to the strong eigenvector V_S is decreasing so much more rapidly than the component corresponding to the weak eigenvector V_W, that solutions travel rapidly along a curve whose slope is similar to that of V_S until the strong eigenvector component of the solution is so small that the rate of change of the weak eigensolution is comparable to that of the strong eigensolution. Once the V_S component is small enough, the weak eigensolution has more of an influence on the solution curve, which then approaches the origin along a curve tangent to the weak eigenline.

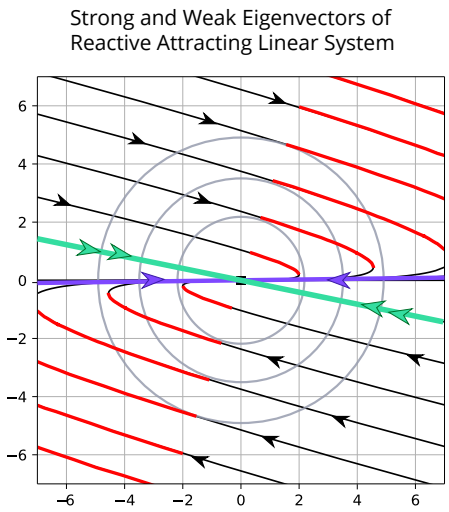

Figure 5.1: The phase plane of the reactive attracting linear system given by Equation 5.1. The strong eigenvector is highlighted in green. The weak eigenvector is highlighted in purple. As solutions are attracted to the weak eigenvector, the pass through the reactive region (in red) where they have positive radial velocity.

We can formalize these radial and tangential dynamics using the radial and tangential velocity framework.

Lemma 5.1. *Consider a reactive attracting system* $\frac{dX}{dt} = AX$ *with eigenvalues* $\lambda_S < \lambda_W < 0$ *and corresponding eigenvectors* V_S *and* V_W*. Then the unique attracting angle of the system (up to modulo* π*) is the angle* θ_W *corresponding to eigenvector* V_W*.*

Proof. Recall that

$$\frac{d\theta}{dt} = \mathcal{T}(\theta). \tag{5.2}$$

Equation 5.2 is an autonomous one-dimensional differential equation for $\theta(t)$ telling us how $\theta(t)$ evolves along solutions $X(t)$ of the autonomous linear system $\frac{dX}{dt} = AX$. By Theorem 4.3, $\mathcal{T}(\theta)$ is sinusoidal with period π. By Lemma 4.7, $\mathcal{T}(\theta)$ has zeros at $\theta_S, \theta_W \in [0, \pi)$ corresponding to eigenvectors V_S and V_W respectively. So θ_S and θ_W are the only equilibria of the θ dynamics (modulo π).

The stability of the equilibria is given by the sign of $\frac{d\mathcal{T}}{d\theta}$. We want to show that when $\theta(t)$ is increasing for θ just below θ_W, and decreasing for θ just above θ_W. That is, we want to show that $\mathcal{T}(\theta) > 0$ for θ just below θ_W, and $\mathcal{T}(\theta) < 0$ for θ just above θ_W. In other words, we want to show $\frac{d\mathcal{T}}{d\theta}(\theta_W) < 0$

By Definition **??**,

$$\frac{d\mathcal{T}}{d\theta} = (a+d) - 2\mathcal{R}(\theta) = tr(A) - 2\mathcal{R}(\theta)$$

Now, $tr(A) = \lambda_S + \lambda_W$. Thus $2\lambda_S < tr(A) < 2\lambda_W$, since $\lambda_S < \lambda_W$. So

$$\frac{d\mathcal{T}}{d\theta}(\theta_W) = tr(A) - 2\mathcal{R}(\theta_W) = tr(A) - 2\lambda_W < 0$$

$$\frac{d\mathcal{T}}{d\theta}(\theta_S) = tr(A) - 2\mathcal{R}(\theta_S) = tr(A) - 2\lambda_S > 0$$

Thus, modulo π, the angle θ_S corresponding to the strong eigenvector V_S is the repelling equilibrium of Equation 5.2, and all other initial values of θ are attracted to θ_W. So for all trajectories of the system $\frac{dX}{dt} = AX$ that are not on the strong eigenline, $\theta(t)$ converges to θ_W □

Lemma 5.2. *Consider a reactive attracting system $\frac{dX}{dt} = AX$ with eigenvalues $\lambda_S < \lambda_W < 0$ and corresponding eigenvectors V_W and V_S. If a solution $X(t) = (r(t), \theta(t))$ has an initial condition $X_0 = (r_0, \theta_0)$ sufficiently close to V_W, then $\frac{dr}{dt}\Big|_{X(t)} < 0$ for all $t > 0$.*

Proof. Let θ_W be the angle corresponding to the weak eigenvector V_W. Consider the solution $X(t) = (r(t), \theta(t))$ with initial condition $X_0 = (r_0, \theta_0)$ sufficiently close to V_W. By the continuity of $\mathcal{R}(\theta)$, there is some sufficiently small distance δ such that

$$|\theta - \theta_W| < \delta \quad \Longrightarrow \quad |\mathcal{R}(\theta) - \lambda_W| < |\lambda_W| = -\lambda_W$$

Suppose that X_0 is sufficiently close to V_W in the sense that $|\theta_0 - \theta_W| < \delta$. Then

$$|\mathcal{R}(\theta_0) - \lambda_W| < -\lambda_W$$

If $\mathcal{R}(\theta_0) < \lambda_W$, then $\mathcal{R}(\theta_0) < 0$. So $\frac{dr}{dt}\Big|_{X_0} = r\mathcal{R}(\theta_0) < 0$.

If $\mathcal{R}(\theta_0) > \lambda_W$, then we can write:

$$\mathcal{R}(\theta_0) - \lambda_W < -\lambda_W$$

Thus $\frac{dr}{dt}\Big|_{X_0} = r_0\mathcal{R}(\theta_0) < 0$.

Recall that by Lemma 5.1, θ_W is an attracting equilibrium of the autonomous one-dimensional equation (5.2). We can therefore choose our original δ sufficiently small so that if $|\theta_0 - \theta_W| < \delta$, then for all $t > 0$,

$$\frac{d}{dt}\big[|\theta(t) - \theta_W|\big] < 0$$

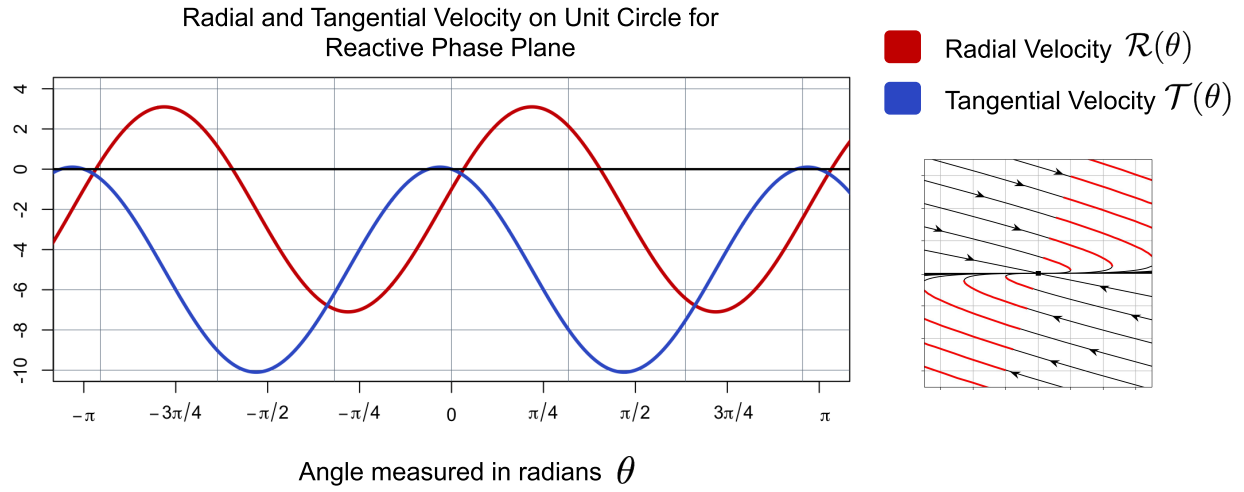

Figure 5.2: The radial and tangential components of the velocity for the reactive attracting system given by Equation 5.1. Noticing that θ-axis is a phase line, we see that solutions attracted to the weak eigenvector from the counterclockwise direction pass through the reactive region where $\mathcal{R}(\theta)$ is positive. Once solutions get close enough to the weak eigenvector, however, $\mathcal{R}(\theta)$ becomes negative again.

This means in particular that

$$|\theta(t) - \theta_W| < |\theta_0 - \theta_W| < \delta$$

Thus, by the same argument we used for θ_0, we can show that $\frac{dr}{dt}\Big|_{X(t)} = r(t)\mathcal{R}(\theta_t) < 0$ for all $t > 0$. □

Seeing how these radial and tangential dynamics play out in the phase plane is supremely helpful in developing intuition about what circumstances give rise to reactivity, and how we might exploit a reactive autonomous system to maintain this positive radial velocity in a non-autonomous system. We see in Figure 5.2 that because of the obtuse angle between the eigenvectors, the positive radial velocity arises as the solutions "seek out" the weak eigenline. Once they get sufficiently close to the eigenline, their radial velocity becomes negative again.

This provides the key to constructing our non-autonomous system. To force a solution to continue having positive radial velocity, we will rotate system (5.1) so that the attracting angle θ_W keeps moving away from the solution curve. We will choose the speed of rotation so that solution curves are trapped in the region of positive radial velocity in pursuit of θ_W,

never getting close enough to regain negative radial velocity, and therefore traveling ever further from the origin.

We therefore construct a non-autonomous linear system by taking the reactive system in Equation 5.1 as a base and conjugating it by time-dependent rotation with rotational velocity κ:

$$\frac{dX}{dt} = A(t)X = \begin{pmatrix} \sin\kappa t & -\cos\kappa t \\ \cos\kappa t & \sin\kappa t \end{pmatrix} \begin{pmatrix} -1 & 10 \\ 0 & -3 \end{pmatrix} \begin{pmatrix} \sin\kappa t & -\cos\kappa t \\ \cos\kappa t & \sin\kappa t \end{pmatrix}^{-1} X \tag{5.3}$$

For each t the matrix $A(t)$ inherits the same eigenvalues as A, and at any instant in time α, the phase portrait of the autonomous linear system

$$\frac{dX}{dt} = A(\alpha)X \tag{5.4}$$

is the phase portrait of system (5.1) rotated counterclockwise by angle $\kappa\alpha$. Since we want the weak eigenvector to rotate in the *clockwise* direction over time, away from the reactive region, we'll choose a rotational velocity $\kappa < 0$.

Now, for the positive radial velocity to accumulate in our construction, we need to choose the rotational speed $|\kappa|$ to be fast enough that solutions can never catch up with $\theta_W(t)$ but slow enough that solutions get stuck in the reactive region of positive radial velocity. The very special structure of our construction allows us to use the radial and tangential approach to determine upper and lower bounds for κ.

To understand the radial and tangential velocities in the non-autonomous system, we change to the frame of reference of the rotating coordinates. In that frame, at each moment in time, the dynamics are given by system (5.1) and the tangential and radial velocities are the same as for system (5.1). However, as the frame rotates, the relative measure of θ is decreased by the amount of rotation, κt, and so the angular velocity $\frac{d\theta}{dt}$ is decreased by κ. In other words, because of the very special structure of our construction and the uniform rotation speed, in the rotating frame of reference the radial and tangential dynamics of the non-autonomous system 5.3 are governed by the autonomous differential equations

$$\begin{aligned} \frac{1}{r}\frac{dr}{dt} &= \mathcal{R}_A(\theta) \\ \frac{d\theta}{dt} &= \mathcal{T}_A(\theta) - \kappa \end{aligned}$$

where $\mathcal{R}_A(\theta)$ and $\mathcal{T}_A(\theta)$ denote the radial and tangential velocities of system (5.1) on the unit circle.

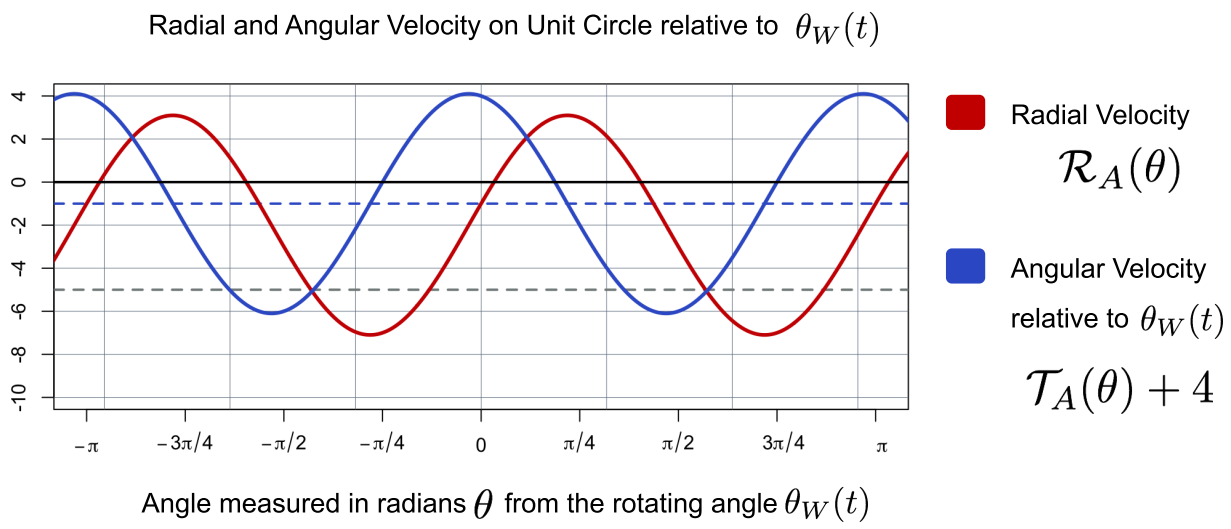

Figure 5.3: Graphs of $\mathcal{R}_A(\theta)$ (red) and $\frac{d\theta}{dt} = \mathcal{T}_A(\theta) + 4$ (blue), where $\mathcal{R}_A(\theta)$ and $\mathcal{T}_A(\theta)$ are the radial and tangential velocities of system (5.1) on the unit circle.

To fix ideas, consider the case when $\kappa = -4$. Figure 5.2 shows the graphs of $\mathcal{R}_A(\theta)$ and $\frac{d\theta}{dt} = \mathcal{T}_A(\theta) + 4$. Now we can apply the same ideas as in the proof of Lemma 5.1 to analyze the tangential dynamics, and then draw conclusions for the radial dynamics.

Whenever $\frac{d\theta}{dt} = 0$, we have an equilibrium angle, in the rotating frame of reference. The angular equilibria correspond to invariant lines in the rotating frame of reference, akin to eigenvectors in autonomous linear systems. When $\kappa = -4$, we find that there are angular equilibria at $\theta = 0.19\pi$ and $\theta = 0.75\pi$. In particular, $\theta^* = 0.19\pi$ is an attracting equilibrium angle since $\frac{d\theta}{dt} < 0$ when $\theta > 0.19\pi$, and $\frac{d\theta}{dt} > 0$ when $\theta < 0.19\pi$.

Because $\theta^* = 0.19\pi$ is the only attracting equilibrium angle (modulo π), the asymptotic radial behavior of almost all solutions to our non-autonomous system are determined by $\mathcal{R}(\theta^*)$. But $\mathcal{R}(\theta^*) > 0$! This is the whole point of our construction! It means that in the rotating frame of reference, solutions with initial angle θ^* move exponentially away from the origin along the invariant line for all time. In other words, θ^* is a direction of repulsion from the origin. Even though the origin is attracting for each instantaneous autonomous snapshot of this non-autonomous system, the transient reactivity accumulates to yield a direction of pure repulsion from the origin.

Almost all other solutions converge to the invariant line with angle θ^*, and hence follow the same motion away from the origin. The only exceptions are solutions with initial angle

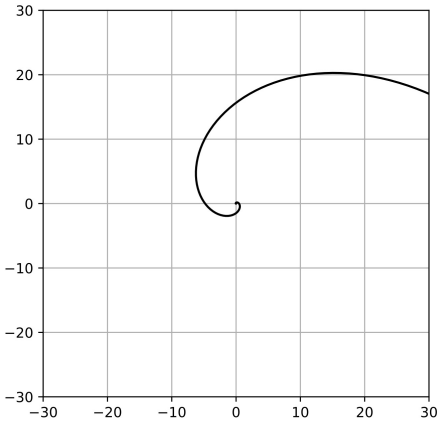

Figure 5.4: System as given in Equation 5.3. Initial value is $X_0 = (0.01, \frac{2\pi}{3})$ in polar coordinates.

at the other equilibrium $\theta = 0.75\pi$. From Figure 5.2, we see that $\mathcal{R}(0.75\pi) < 0$, and hence solutions are attracted to the origin along this invariant line in the rotating frame of reference.

The repelling behavior also confirmed through numerical simulation. Figure 5.2 shows the solution flow obtained by simulating the system for initial value X_0 with polar coordinates $(0.01, \frac{2}{3}\pi)$. The solution spirals away from the origin in the fixed frame of reference of the coordinate axis, corresponding to convergence to the invariant line of repulsion in the rotating frame of reference.

We now have an example of a non-autonomous linear system in which the reactivity accumulates to yield trajectories of pure repulsion from the origin even though each of its instantaneous autonomous systems is asymptotically attracting.

The next question is, can we observe this same repulsion when we consider the time-τ map of this non-autonomous linear system? Certainly, yes! In the rotating frame of reference, we have a direction of pure repulsion and a direction of pure attraction. The time τ map is the linear autonomous map that results from following these dynamics over the time interval $[0, \tau]$. Thus in the rotating frame of reference for one iteration of time-τ, $\theta = 0.19\pi$ is an eigendirection with eigenvalue $|\lambda| > 1$ and $\theta = 0.75\pi$ is an eigendirection with eigenvalue $|\lambda| < 1$. The eigenvalues and thus the stability classification persist in the fixed frame of reference. Thus the origin is a saddle for the autonomous, linear time-τ map.

This is show through simulation for $\tau = \frac{9\pi}{32}$. By Lemma 2.6, we know that the time-τ

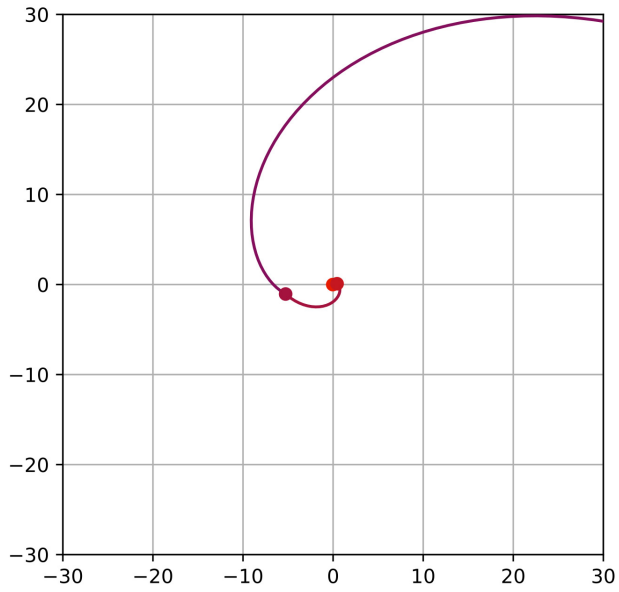

Figure 5.5: The orbit generated from the time-$\tau = \frac{9\pi}{32}$ map of the system given in Equation 5.3 with seed $X_0 = (0.01, \frac{2\pi}{3})$ in polar coordinates.

map of any non-autonomous linear system is a linear transformation. Thus we can find a matrix representation of the time-τ map and confirm the asymptotic stability we observe by checking the eigenvalues.

Simulating this system using standard numerical methods, we find that

$$U_\tau\left(\begin{pmatrix}1\\0\end{pmatrix}\right) \approx \begin{pmatrix}-9.998\\-2.001\end{pmatrix}$$

and

$$U_\tau\left(\begin{pmatrix}0\\1\end{pmatrix}\right) \approx \begin{pmatrix}-9.997\\-2.003\end{pmatrix}$$

Thus the time-τ map can be represented via

$$U_\tau(X) \approx \begin{pmatrix}-9.998 & -9.997\\-2.001 & -2.003\end{pmatrix} X$$

The eigenvalues of this matrix are $\lambda_1 = -1.100$ and $\lambda_2 = -0.002$. Since $|\lambda_1| > 1$ and $|\lambda_2| < 1$, by the criteria for discrete systems outlined in Table 3.1, the origin is a saddle equilibrium of the discrete linear system generated by the time-τ map of Equation 5.3.

We now have an example of a non-autonomous linear system for which the time-τ map is unstable even though each of its instantaneous linear systems have negative eigenvalues. Thus we have an example that shows that it *is* possible for the reactive positive radial velocity of attracting linear systems can accumulate to exhibit instability if strung along in a non-autonomous linear system for $t \in [0, \tau]$.

5.3 Return to Conjecture 3.5, and Moving Forward

In Section 5.2, we were able to construct an example of a non-autonomous system whose time-τ map has asymptotic behavior that differs from the asymptotic behavior of each instantaneous linear system that composes it. The existence of a non-autonomous system with these properties confirms that the distinction between transient and asymptotic behavior *is* significant in the context of classifying the stability of time-τ maps of non-autonomous linear systems. We now have evidence that stringing along the asymptotic classification of instantaneous linear systems is not enough to classify their cumulative non-autonomous dynamics.

The non-autonomous example we constructed does not, however, disprove Conjecture 3.5. To use this example as a counterexample for our conjecture, we would need to prove that it can arise as the variational equation of a flow-kick equilibrium trajectory for some system $\frac{dX}{dt} = F(X)$, flow time τ, and equilibrium trajectory $\gamma(t, X^*)$. It is not obvious whether there exists a flow-kick system for which the variational equation can have this pattern of rotation, and, if such a flow-kick system *does* exist, it is not obvious how to find it.

One reason why determining whether Equation 5.3 can arise as a variational equation is a non-trivial task is because of the constraints on the composition of a variational equation. For a non-autonomous linear system $\frac{dX}{dt} = A(t)X$ to be a variational equation, we need the following criteria to be met:

(i) There exists a vector field $F \in C^1$ such that for all $\alpha \in [0, \tau]$, $A(\alpha) = D[F(X)]$ for some $X \in \mathbb{R}^n$.

(ii) Given the function $X(t)$ that describes the points $X(\alpha)$ such that for all $\alpha \in [0, \tau]$, $A(\alpha) = D[F(X(\alpha))]$, $X(t)$ must be a solution curve $\phi(t, X_0)$ of $\frac{dX}{dt} = F(X)$ on $t \in [0, \tau]$ for some initial condition $X_0 = X(0) \in \mathbb{R}^n$.

These seem to be strict criteria that, at the very least, make it hard to prove that a non-autonomous linear system like Equation 5.3 *is* a variational equation. In fact the criteria seem to be strict enough that they would impose a particular structure on variational equations that may constrain the dynamic behavior. The questions arises: do these criteria preclude the type of dynamic behavior that would allow for accumulated transient behavior that differs from the asymptotic behavior at every instant?

We can start exploring the answer to this question by first breaking it into smaller, but no less significant, questions:

- What kind of behavior do we observe in the variational equations of flow-kick systems that we can simulate?
- What kind of behavior can we observe in variational equations for which the each instantaneous linear approximation exhibits very positive reactivity?
- What kind of structures can we determine preclude the accumulation of transient behavior that differs from the asymptotic behavior?
- The one example we have constructed of a non-autonomous linear system that accumulates reactivity uses pure rotation. Are there other non-autonomous structures that can allow for this accumulation?

To move forward in answering these questions, we are using numerical simulation (as described in Section 3.1) to help build our intuition about what can happen in the variational equation, and what seems not to happen in the variational equation. As we build up a library of observations to address the first two questions, we will begin to develop analytic intuition that will guide our exploration of the last two questions.

Though this phase of research is still ongoing, preliminary numerical observations show that for flow-kick systems in which the underlying differential equation is a Lotka-Voltera competition model (as in Example 3.4), even for equilibrium trajectories whose associated attracting instantaneous linearizations have great amounts of reactivity, the variational time-τ map is attracting. Instead of observing unstable variational time-τ maps, we have observed partial accumulation of reactivity leading to *reactive* variational time-τ maps.

These preliminary results seem to suggest that, at least in Lotka-Voltera competition models, accumulated reactivity can lead to *reactive* but not *unstable* variational time-τ maps.

However, much work remains to be done before determining that this idea can be supported analytically.

Bibliography

[1] Abdel-Rady, A.S., El-Sayed, A. M. A., Rida,S. Z., & Ameen I. (2012) On some impulsive differential equations Math. Sci. Lett. 1 No. 2, 105-113

[2] Argarwal, R., et.al.(2017) Non-Instantaneous Impulses in Differential Equations. Springer International Publishing AG 2017. DOI 10.1007/978-3-319-66384-5_1

[3] Bradley, L. (1999). The Variational Equation: Notes for CSCI 4446/5446. Department of Computer Science University of Boulder Colorado. `https://www.cs.colorado.edu/ lizb/chaos/variational-notes.pdf`

[4] Brettin, A. (2019) Ecological management strategies for grasslands informed by flow-kick dynamics. (Undergraduate Thesis for the University Honors Program at University of Minnesota Twin Cities).

[5] Hirsch, M. W., Smale, S., & Devaney, R. L. (2012). Differential equations, dynamical systems, and an introduction to chaos (3rd ed.). Cambridge, MA: Academic Press.

[6] Horn, R.A., Johnson, C.R. (2013). Matrix Analysis (2nd ed.). New York, NY: Cambridge University Press.

[7] IPCC, 2013: Summary for Policymakers. In: Climate Change 2013: The Physical Science Basis. Contribution of Working Group I to the Fifth Assessment Report of the Intergovernmental Panel on Climate Change [Stocker, T.F., D. Qin, G.-K. Plattner, M. Tignor, S.K. Allen, J. Boschung, A. Nauels, Y. Xia, V. Bex and P.M. Midgley (eds.)]. Cambridge University Press, Cambridge, United Kingdom and New York, NY, USA.

[8] Lee, V. (2016). Exploring resilience: the dynamics of linear and non-linear flow-kick systems. (Bowdoin College Honors Thesis 2016 L44). Special Collections and Archives, Bowdoin College, ME.

[9] Meyer, K., Hoyer-Leitzel, A., Iams, S., Klasky, I. J., Lee, V., Ligtenberg, S., Bussmann, E., Zeeman, M. L. (2018). Quantifying resilience to recurrent ecosystem disturbances using flow-kick dynamics. Nature Sustainability.

[10] Neubert, M.G., Caswell, H. (1997). Alternatives to resilience for measuring the responses of ecological systems to perturbations. Ecology, 78(3), 653-665.

[11] Zeeman ML, Meyer K, Bussmann E, et al. (2018) Resilience of socially valued properties of natural systems to repeated disturbance: A framework to support value-laden management decisions. Natural Resource Modeling. 2018;e12170. https://doi.org/10.1111/nrm.12170